The Proceedings of the 5th International Symposium on Radiation Emergency Medicine at Hirosaki University

The 2013
Hirosaki University
International Symposium

The 5th International Symposium on Radiation Emergency Medicine at Hirosaki University

Organized by
Hirosaki University Graduate School of Health Sciences
Hirosaki University Institute of Radiation Emergency Medicine
Hirosaki University Education Program for Professionals in Radiation Emergency Medicine
Sponsored by
The Radiological Nursing Society of Japan

Contents

Poster Presentation

1) Department of Biomedical Sciences, Division of Medical Life Sciences, Hirosaki University Graduate School of Health Sciences
2) Department of Medical Technology, Hirosaki University School of Health Sciences
3) Research Center for Biomedical Sciences, Hirosaki University Graduate School of Health Sciences

Special Symposium

Gene expression analyses of messenger RNA and non-coding RNA in human lymphoblastic cells exposed to X-ray

Mitsuru Chiba[1*], Tomisato Miura[2], Kosuke Kasai[2], Satoru Monzen[3], Naoki Nanashima[1], Takashi Ishikawa[1], Teruko Takeo[1], Ikuo Kashiwakura[3], and Toshiya Nakamura[1]

[1] Department of Biomedical Sciences, Division of Medical Life Sciences, Hirosaki University Graduate School of Health Sciences, 66-1 Hon-cho, Hirosaki, Aomori, 036-8564, Japan
[2] Department of Pathologic Analysis, Division of Medical Life Sciences, Hirosaki University Graduate School of Health Sciences, 66-1, Hon-cho, Hirosaki, Aomori, 036-8564, Japan
[3] Department of Radiological Life Sciences, Division of Medical Life Sciences, Hirosaki University Graduate School of Health Sciences, 66-1, Hon-cho, Hirosaki, Aomori, 036-8564, Japan

Abstract. Ionizing radiation (IR) causes deoxyribonucleic acid (DNA) injury and activates intracellular signaling pathways, including pathways involved in regulating DNA repair and cell cycle. However, further knowledge of the molecular events subsequent to radiation exposure is essential to more comprehensively understand its effects. Therefore, we investigated the gene expression of messenger ribonucleic acid (mRNA) and *cis*-natural antisense transcripts (*cis*-NATs) (a class of non-coding RNA) in a human B lymphoblast cell line (IM-9) following X-ray irradiation. The expression analyses were performed using a microarray system and reverse transcription quantitative polymerase chain reaction (RT-qPCR). Microarray analysis revealed the mRNA expressions of 94 genes were up-regulated >1.5-fold in irradiated cells (4 Gy), as compared to non-irradiated cells (0 Gy). Among 94 genes, the majority of genes were up-regulated by X-ray irradiation in a dose-dependent manner. When strand-specific RT-qPCR was performed using complementary DNA (cDNA) synthesized from strand-specific RNA, the expression levels of *MDM2* and *CDKN1A* mRNA were found to be significantly up-regulated in an X-ray dose-dependent manner. Interestingly, the expressions of their *cis*-NATs were also up-regulated proportional to X-ray dose. This is the first report to demonstrate the expression of *cis*-NATs from these genes. These results indicate that irradiation-induced up-regulation of the mRNA and *cis*-NATs from these genes may represent future biological dosimetric markers for evaluating radiation exposure.

Key Words: radiation, gene expression, B lymphoblast cells, *MDM2*, *CDKN1A*, non-coding RNA

[*] Corresponding to: Mitsuru Chiba, Lecturer, Hirosaki University, 66-1 Hon-cho, Hirosaki, Aomori, 036-8564, Japan.
E-mail: mchiba32@cc.hirosaki-u.ac.jp

Introduction

Recent studies have revealed that IR generates reactive oxygen species (ROS) and reactive nitrogen species (RNS) in cells, which leads to DNA injury at random sites. Poly (ADP-ribose) polymerase (PARP) and DNA-dependent protein kinase repair complex (DNA-PK) are activated by DNA double-strand breaks (DSB) to effect DNA repair [1]. In addition, ataxia telangiectasia mutated (ATM) is activated in response to DNA injury and initiates phosphorylation of p53, which has been found to up-regulate mRNA expression of *GADD45*, *MDM2*, *CDKN1A* ($p21^{Cip1}$), and *BAX* to control cell cycle, DNA repair, and apoptosis [1].

Recently, a large number of non-coding RNAs, which are not translated into proteins, have been discovered using transcriptome analysis. Currently, non-coding RNAs are sub-classified into microRNA, Piwi-interacting RNA (piRNA), small nuclear RNA (snRNA), and natural antisense transcripts (*cis*-NATs) transcribed from DNA strands opposing the sense strands [2]. It has been demonstrated that *cis*-NATs are involved in the control of eukaryotic gene expression [2, 3]. In the present study, mRNAs and *cis*-NATs up-regulated by X-ray irradiation were investigated in the human B lymphoblastic cell line (IM-9) which is highly sensitive to IR.

Materials and methods

X-ray irradiation.

The IM-9 (JCRB0024) was purchased from the Health Science Research Resources Bank (Osaka, Japan). The IM-9 cells were cultured in RPMI-1640 medium supplemented with 10% fetal bovine serum, 100 units/ml penicillin, and 100 μg/ml streptomycin at 37˚C in an atmosphere of 5% CO_2. The IM-9 cells were seeded onto 6-well plates at a concentration of 2 x 10^5 cells/well for X-ray irradiation experiments.

The IM-9 cells plated on the wells were cultured as described above for 24 h prior to X-ray irradiation. Irradiation (150 kVp, 20 mA, 0.5-mm aluminium and 0.3-mm copper filters) was performed using an X-ray generator (MBR-1520R-3; Hitachi Medical Corporation, Tokyo, Japan) at a distance of 45 cm between the focus and the target. The dose rate was 80 cGy/min. The dose was monitored with a thimble ionization chamber that was placed next to the sample during the irradiation. The irradiated cells were further cultured for 24 h under the same conditions, and then collected by centrifugation. The cells thus collected were frozen in liquid nitrogen and stocked at -80˚C until being used for RNA extraction.

Microarray analysis.

Cyanine 3 (Cy3)-labeled cDNA was synthesized from 10 μg total RNA (irradiated or non-irradiated samples) using a LabelStar Array kit (Qiagen), Cy3-dUTP (GE healthcare), and random nonamer primers. Agilent 44 K x 4 human custom-microarray slides were hybridized with the Cy3-labeled cDNA (2 μg) in a hybridization solution (In Situ Hybridization Kit Plus, Agilent Technologies), following the manufacturer's instructions.

Strand-specific RT-qPCR.

Total RNAs were subjected to synthesis of first-strand cDNA from mRNA or *cis*-NATs using reverse or forward primers and Reverse Transcriptase (Promega) together with the *ACTB* (β-actin) reverse primer. The mixtures were then incubated at 50°C for 60 min. The first-strand cDNAs derived from mRNA or *cis*-NATs were used as a template for quantitative PCR (qPCR) using the Power SYBR Green PCR Master Mix (Applied Biosystems). qPCRs were performed using the Applied Biosystems StepOne Plus Real-Time PCR system at 95°C for 10 min followed by 40 cycles each of 95°C for 15 sec and 60°C for 60 sec. In order to compare the PCR results, the values for mRNA and *cis*-NATs were normalized based on the values of *ACTB* mRNA.

Results and discussion

Microarray analysis showed that the expression of 94 mRNAs were up-regulated more than 1.5 times in the irradiated samples (4 Gy), as compared to non-irradiated samples (0 Gy) (data not shown). Among the 94 mRNAs, *MDM2* and *CDKN1A* mRNAs were up-regulated by X-ray exposure in a dose-dependent manner (Table 1). The mRNAs and *cis*-NATs of *MDM2* and *CDKN1A* were found to be up-regulated in proportion to X-ray exposure by strand-specific RT-qPCR (Figure 1). In conclusion, radiation-responsive *cis*-NATs were identified for the first time. *MDM2* and *CDKN1A* are p53-related genes involved in DNA repair and cell cycle regulation. It is expected that these *cis*-NATs exert post-transcriptional regulation of mRNA expression.

In the future, IR dose-dependent up-regulation of these mRNAs and *cis*-NATs may be used as biomarkers for evaluating DNA injury.

Acknowledgments

This study was supported by a grant from the Hirosaki University Graduate School of Health Sciences Radiation Emergency Medicine Human Resource Cultivation Project.

References

[1] Bourguignon MH, Gisone PA, Perez MR, et al.: Genetic and epigenetic features in radiation sensitivity Part I: cell signalling in radiation response. Eur J Nucl Med Mol Imaging 32: 229-246, 2005.

[2] Lavorgna G, Dahary D, Lehner B, Sorek R, Sanderson CM and Casari G: In search of antisense. Trends Biochem Sci 29: 88-94, 2004.

[3] Werner A and Berdal A: Natural antisense transcripts: sound or silence? Physiol Genomics 23: 125-131,

Table 1. *MDM2* and *CDKN1A* mRNAs up-regulated more than 1.5 times compared to 0 Gy after IR exposure in IM-9 cells.

Gene symbol	Accession no.	Relative expression ratio (vs 0 Gy)				Gene name
		0 Gy	1 Gy	2 Gy	4 Gy	
MDM2	NM002392.2	1.00	1.91	2.30	3.49	Mdm2, transformed 3T3 cell double minute 2, p53 binding protein (mouse)
CDKN1A	NM078467.1	1.00	1.83	2.15	2.96	cyclin-dependent kinase inhibitor 1A (p21, Cip1)

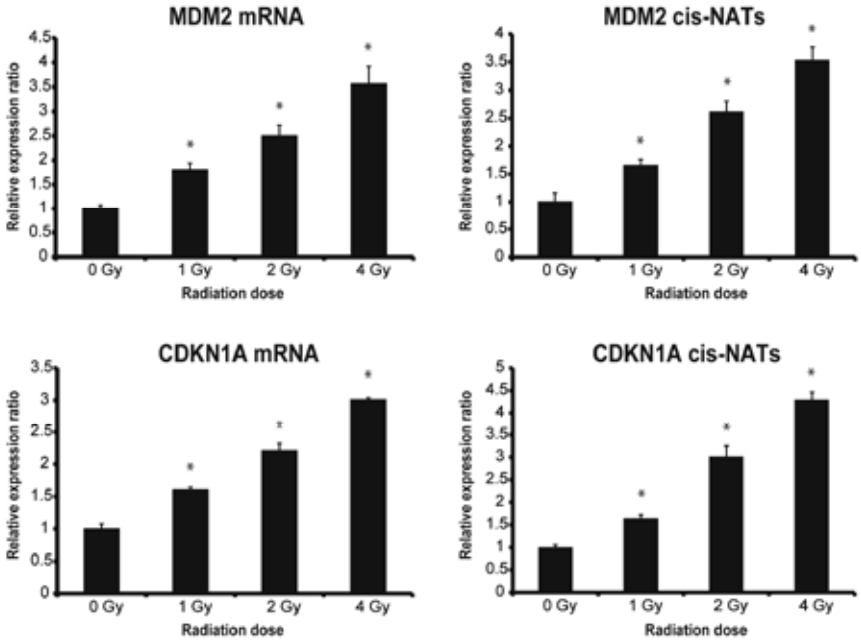

Figure 1. Relative expression of mRNAs and NATs of *MDM2* and *CDKN1A* genes in X-ray irradiated IM-9 cells.
The mRNA and NAT expression levels were determined using strand-specific RT-qPCR analysis. Values for mRNAs and NATs were normalized based on *ACTB* mRNA levels. Asterisks indicate statistical significance, compared with 0 Gy ($p < 0.05$).

Morphological studies of the skin and its derivatives, bone marrow, lymph node, and other organs in X-irradiation mice

Shoji Chiba[1]*, Syuji Fukushima[2], Yuhei Nakamura[3], Shota Sato[4], Koichi Itoh[5], Manabu Nakano[5] and Haruhiko Yoshioka[1]

Departments of [1]Pathologic Analysis and [5]Biomedical Sciences, Division of Medical Life Sciences, Hirosaki University Graduate School of Health Sciences

[2]Kitahara International Hospital

[3]Hospital Hakodate Hokkaido

[4]Student in Department of Radiological Technology, Hirosaki University School of Health Sciences

Abstract. To morphologically confirm acute radiation damage and organ radiosensitivity in mice, we performed whole body X-ray irradiation at single doses of 0 (control), 2, 4, 8, and 10 Gy. X-ray irradiation (8 to 10 Gy) causes a decrease in the number of lymphocytes in the submandibular lymph node, as well as in the number of progenitor cells for leukocytes and lymphocytes. X-ray irradiation also causes a decrease in the number of megakaryocytes in the bone marrow of males and females exposed to doses of 8 and 10 Gy, but not to erythrocytes, reticular, or fat cells. The number of lymphocytes in the lymph node, progenitor cells, and megakaryocytes in the bone marrow decreased significantly following exposure to 4 Gy. No differences in morphological appearance were found between exposed and control mice in skin and its derivatives (sweat and sebaceous glands, hair, and nail), incisor tooth, the ducts for generative organs (uterus, ductus deferens, seminary gland, and spongy urethra), hypophysis, skeletal muscles (masseter and gastrocnemius), and cartilaginous and osseous tissues.

Key Words: acute X-radiation damage, submandibular lymph node, bone marrow, morphology, mouse

Introduction

Textbooks on radiation describe acute injuries to tissues and cells when organs are exposed to X-ray irradiation [1]. The present study was conducted to confirm previously documented morphological damage from X-ray irradiation in skin, bone marrow, submandibular lymph nodes, incisor tooth, skeletal muscles, hypophysis and the ducts for generative organs in mice.

Materials and Methods

The whole bodies of 7-week-old ICR mice (2 males and 2 females; 2 exposed to each dose in the A and C series) were exposed to 2, 4, 8 and 10 Gy of X-ray irradiation generated using a Hitachi MBR-1505R2 (at the Institute for Animal Experiments of Hirosaki University) at a dose rate of 0.133 Gy/min. Ten days after X-ray irradiation, the mice were sacrificed and stored in 10% formalin [2]. These irradiations were conducted in 2010.

We prepared samples of skin and its derivatives from throughout the body, excluding the tail and fingers, and samples from the submandibular lymph node, hypophysis, skeletal muscles and ducts for generative organs. Samples were sliced into 5-μm thick sections and were subjected to hematoxylin and eosin (H & E) staining in 2012. Samples were

prepared from cartilage from various parts of the body, from osseous organs with bone marrow, from tail and fingers, and from incisor tooth; these samples were sliced into 10-μm sections following decalcification using the Plank and Rychlo method [3], and were subjected to H & E staining. Digital photographs of the H & E staining sections were obtained under a light microscope to detect morphological changes in the tissues.

Results

1. Skin and its derivatives

Skin (head, ear, nose, abdomen and digital pad) consisted of the basal, spinous, granular and cornified layers. For all skin samples, the basal layer consisted of one layer of cuboidal cells (Figs. 1a–4b). For many of the skin samples, the spinous layer consisted of one or two layers of squamous cells; however, it consisted of three or four layers in samples obtained from the tail and the palm of the second finger (Figs. 3a, b) and of about ten layers of spindle-like cells in samples obtained from the digital pad of the second finger (Figs. 4a, b). In many of the skin samples, the granular layer consisted of one or two layers of squamous cells with small areas of black pigment (Figs. 1a-4b). In all these samples, the three layers of skin and the cells comprising these layers were similar in mice exposed to 0 and 10 Gy.

In all the skin derivative samples, hairs were found to originate from hair follicles and bulbs in the corium and the subcutaneous tissue (Figs. 3a, 5), and sinus hairs were found to develop from large hair bulbs in the nose. The sebaceous gland was located around the root of the hair and the cytoplasm of mature cells was found to have broken down and nucleus for holocrine secretion (Figs. 1a, b). Sweat glands are situated only in the digital pad of the fingers. The terminal portion and excretory duct of the sweat glands were found to be covered with a simple cuboidal epithelium (Fig. 6). The nail root develops from the nail matrix and is attached to the distal phalanx, in which the columnar cells changed into squamous cells, and the nail body was filled with keratin (Fig. 7). The histological features of the skin derivatives mentioned above were similar in mice exposed to either 0 or 10 Gy.

2. Submandibular lymph node

In the submandibular lymph node, the number of leukocytes decreased at 4 Gy, and most had disappeared following exposure to 8 and 10 Gy [3], whereas reticular cells survived (Figs. 8a, b). It was difficult to distinguish lymphatic nodules from the medulla in the lymph node (Figs. 9a, b).

3. Bone marrow, bones, cartilage, and incisor tooth

Bone marrow in the thoracic and coccygeal vertebrae [3], sternum, temporal bone and condyle of the femur showed that many progenitor cells for leukocytes and lymphocytes, and megakaryocytes had completely disappeared in the medullary cavities following exposure to 8 and 10 Gy. Many progenitor cells in the bone marrow started to disappear at 4 Gy. Only erythroblasts and their derivatives survived with the reticular cells. Following a dose of 10 Gy, half the erythroblasts and their derivatives disappeared following exposure to 8 Gy (Figs. 10a–d). In the coccyx, the bone marrow was filled with many fat cells. Few progenitor cells were seen near the erythrocytes in coccygeal bones dosed at 8 and 10 Gy and in temporal bone dosed at 8 Gy (Figs. 11a–d). In the osseous tissues, the inner surface was covered with a layer of osteoblasts and osteocytes situated in the bone cavities (Figs. 10a–11d).

In the knee joint, the articular cartilage of the patella and femur condyle consisted of a simple squamous layer and 3–4 layers of small cartilaginous cells (Fig. 12). The costal cartilage consisted of three layers: the perichondrium of about 7–8 squamous cells, several chondroblasts, and many chondrocytes in the cartilage cavities (Fig. 13). In incisor tooth, the dental pulp was covered with a layer of odontoblasts, and many dentinal tubules in the dentine ran parallel or oblique to the dental pulp (Fig. 14). The periodontal membrane is situated between the dental alveolus and the radix dentis. The cementoblasts covered a black and thin layer of cement over the dentin, and Sharpey's fibers penetrated a layer of osteoblasts over the dental alveolus into the external basic lamellae of the mandible (Fig. 15).

In front of the nasal cavity, the mucosa was covered with a keratinized stratified squamous epithelium. No particular changes were observed in cartilage from the ear and nose following doses of 0 or 10 Gy (Figs. 2a, 2b, 16).

The histological features of various bones, cartilage, and incisor tooth were similar in mice exposed to either 0 or 10 Gy.

4. Skeletal muscles

In transverse sections of the masseter and gastrocnemius, large diameter muscle fibers (fast fiber) were about four times more common than small muscle fibers (slow fiber) (Fig. 17). No morphological changes were seen between the non-exposed and exposed mice.

5. Ducts for generative organs

The uterus consisted of three layers (endometrium, myometrium, and perimetrium). The uterine glands situated in the functional layer of the endometrium have a simple columnar epithelium (Fig. 18).

The ductus deferens consisted of three layers (mucosa, three layers of smooth muscle, and adventitia). The mucosa was covered with a pseudostratified ciliated epithelium (Fig. 19). The seminal vesicles consisted of mucosa with incomplete folds covered with a simple columnar epithelium in the cavity, smooth muscle, and adventitia. Secretion materials filled the cavity (Fig. 20). The preputial gland consisted of many sebaceous glands. The cavities were enveloped in a simple squamous epithelium and filled with fat (Fig. 21). The spongy urethra consisted of mucosa covered with a transitional epithelium (three or four layers of cells), many veins and trabeculae, and the tunica albuginea (Fig. 22).

In the ducts for generative organs, no morphological differences were seen following doses of 0 or 10 Gy.

6. Hypophysis and membranous labyrinth

The pars anterior of the hypophysis consisted of three cell types (acidophil, basophil, and chromophobe). No cellular degeneration was seen at a dose of 10 Gy (Fig. 23).

In this study, for the membranous labyrinth in the temporal bone, we could not obtain good sections through the cochlear duct and the crista ampullaris of the semicircular ducts.

Discussion

No differences were found in the morphological appearance of skin and its derivatives, incisor tooth, the ducts for generative organs, hypophysis, skeletal muscles, and cartilaginous and osseous tissues between non-exposed and exposed mice.

X-ray irradiation causes a decrease in the number of lymphocytes in the submandibular lymph node, as well as a decrease in the number of cells in the bone marrow. Lymphocytes in the lymph node and progenitor cells for leukocytes in bone marrow are extremely sensitive to X-ray irradiation, as mentioned in many textbooks on radiology [1].

References

[1] Masuda K, Sasaki H. Radiobiology (in Japanese). Tokyo: Nanzando. (1996)

[2] Chiba S, Kagamiya M, Itoh K, et al. Acute X-irradiation damages to the appearances and some visceral organs in mice. Proc. of 2nd Intern. Symp. Rad. Emerg. Med. at Hirosaki Univ. 85-92 (2011).

[3] Chiba S, Higuchi Y, Nakai T, et al. Morphological study of the digestive, nervous and sensory organs, bone marrow, and lymph node in X-irradiation mice. Proc. of 4th Intern. Symp. Rad. Emerg. Med. at Hirosaki Univ. 81-87 (2013).

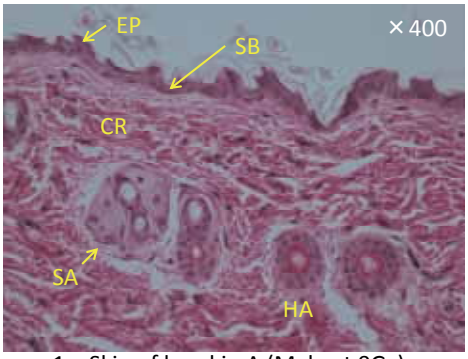

1a. Skin of head in A (Male at 0Gy)

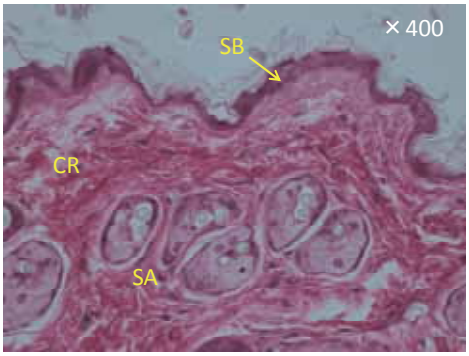

1b. Skin of head in A (Male at 10Gy)

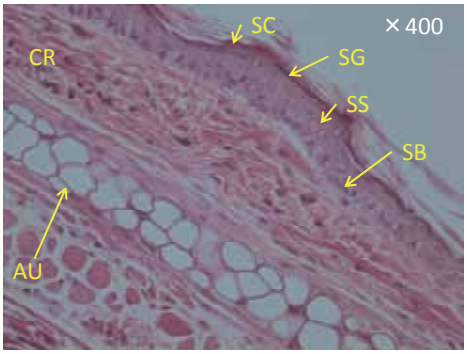

2a. Skin of ear in A (Male at 0Gy)

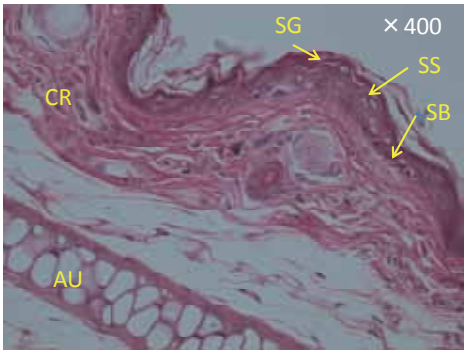

2b. Skin of ear in A (Male at 10Gy)

Figs. 1a-2b. Sections of skin from the head and ear. H&E staining. Magnification 400×. AU, auricular cartilage; CR, corium; EP, epidermis; HA, hair; SA, sebaceous gland; SC, stratum corneum; SG, stratumgranulosum; SS, stratum spinosum.

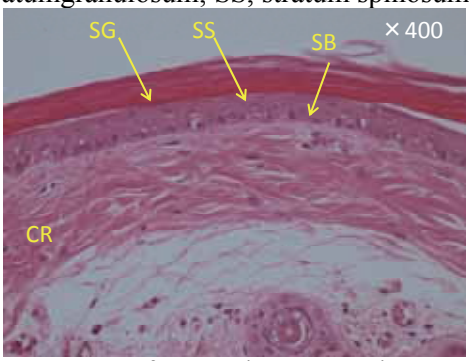

3a. Skin of tail in A (Male at 0Gy)

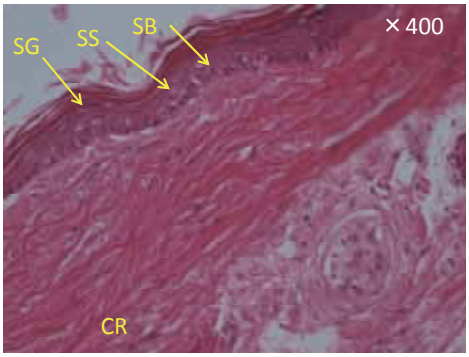

3b. Skin of tail in A (Male at 10Gy)

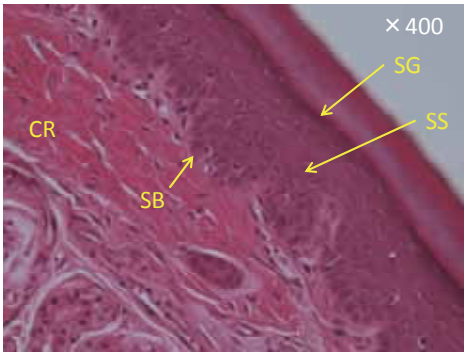

4a. Skin of digital pad in A (Male at 0Gy)

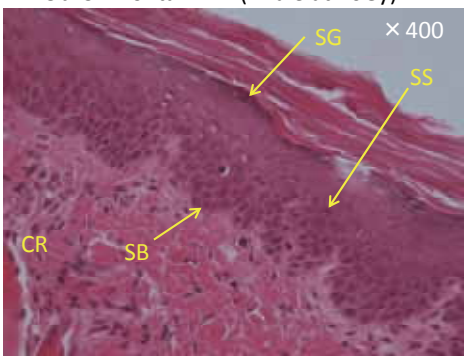

4b. Skin of digital pad in A (Male at 10Gy)

Figs. 3a-4b. Sections of skin from the tail and digital pad. H&E staining. Magnification 400×. CR, corium; EP, epidermis; SG, stratum granulosum; SS, stratum spinosum.

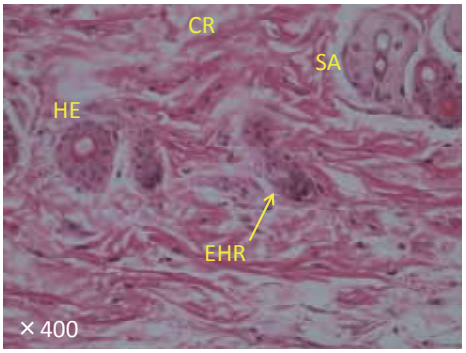

5. Hair of head in C (Female at 10Gy)

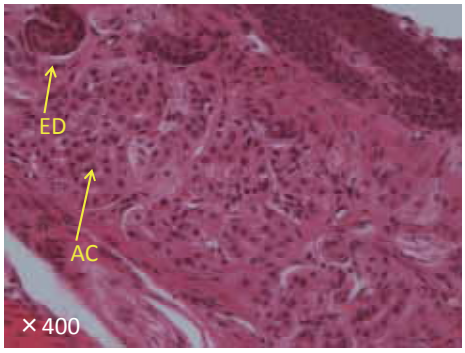

6. Sweat gland in A (Male at 10Gy)

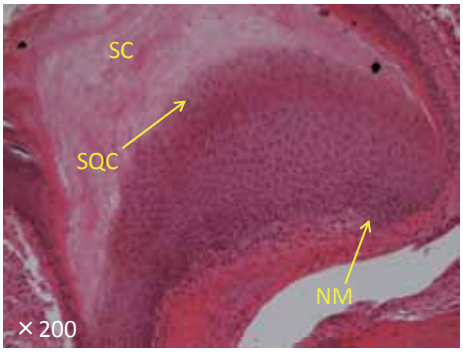

7. Nail in A (Male at 10Gy)

Figs. 5-7. Sections of hair, sweat gland, and nail. H&E staining. Magnifications 400× and 200×. AC, acinus; CR, corium; ED, excretory duct; ERS, external root sheath; HA, hair; NM, nail matrix; SC, stratum corneum; SQC, squamous cell; SW, sweat gland.

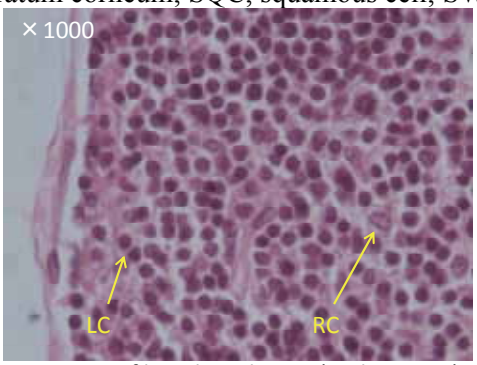

8a. Cortex of lymph node in C (Male at 0Gy)

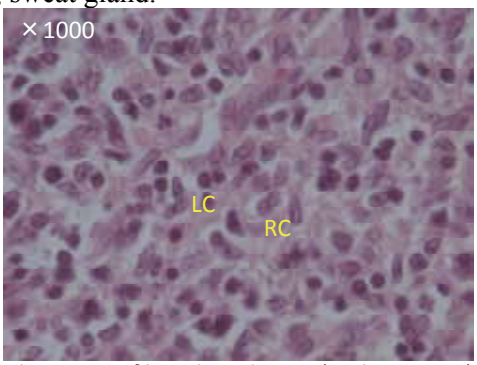

8b. Cortex of lymph node in C (Male at 10Gy)

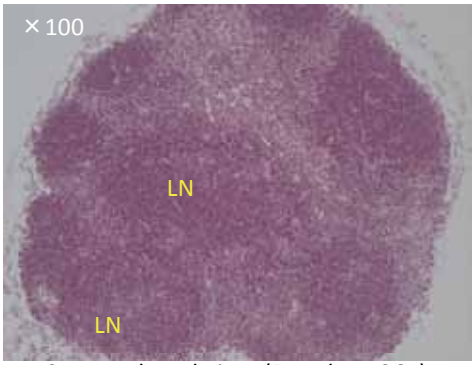

9a. Lymph node in A (Female at 0Gy)

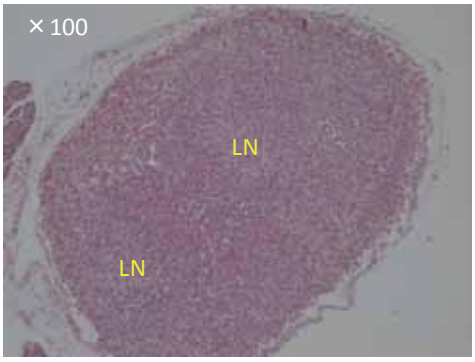

9b. Lymph node in A (Female at 10Gy)

Figs. 8a-9b. Sections of submandibular lymph nodes and their cortex. H&E staining. Magnifications 1000× and 100×. LC, lymphocyte; LN, lymphoid follicle; RC, reticular cell.

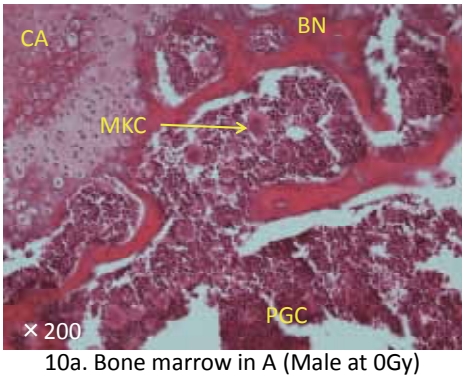

10a. Bone marrow in A (Male at 0Gy)

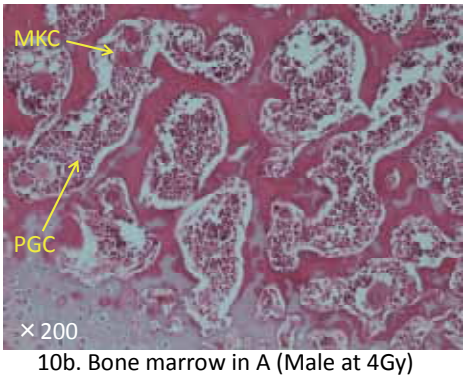

10b. Bone marrow in A (Male at 4Gy)

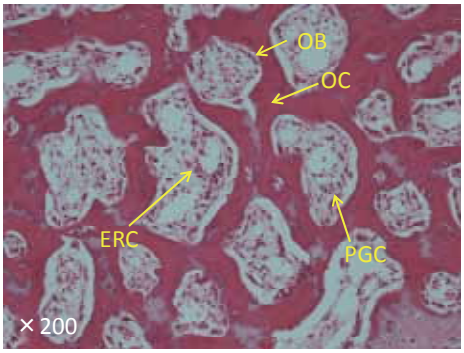

10c. Bone marrow in A (Male at 8Gy)

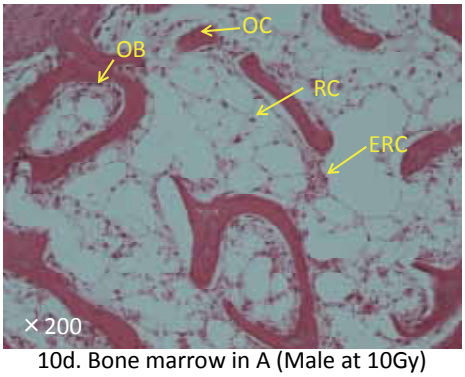

10d. Bone marrow in A (Male at 10Gy)

Figs. 10a-d. Sections of sternum and its bone marrow. H&E staining. Magnification 200×. BN, bone; CA, cartilage; ERC, erythrocyte; MKC, megakaryocyte; OB, osteoblast; OC, osteocyte; PGC, progenitor cells for leukocytes and lymphocytes; RC, reticular cell.

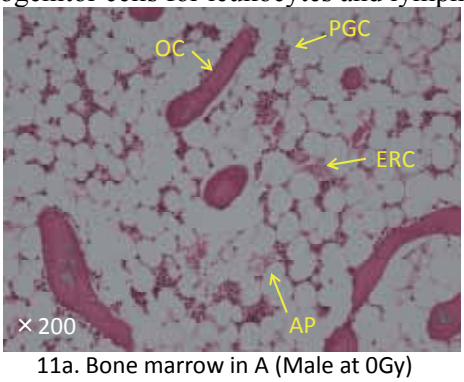

11a. Bone marrow in A (Male at 0Gy)

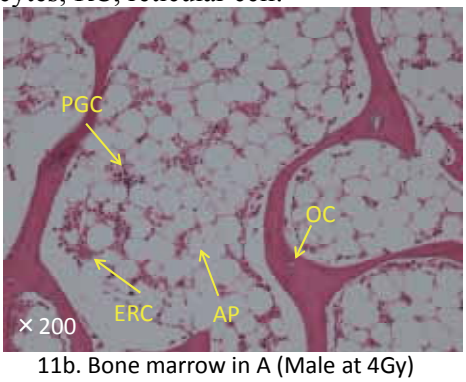

11b. Bone marrow in A (Male at 4Gy)

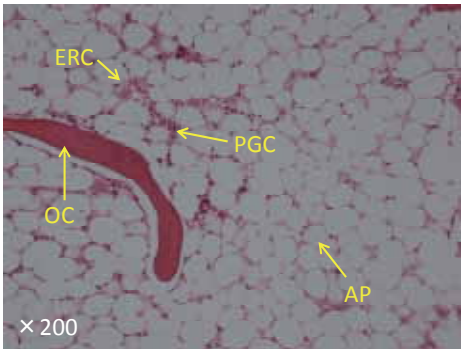

11c. Bone marrow in A (Male at 8Gy)

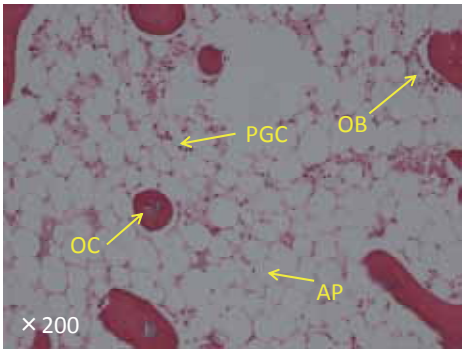

11d. Bone marrow in A (Male at 10Gy)

Figs. 11a-d. Sections of coccygeal vertebra and its bone marrow. H&E staining. Magnification 200×. AP, adipose cell; ERC, erythrocyte; OB, osteoblast; OC, osteocyte; PGC, progenitor cells for leukocytes and lymphocytes; RC, reticular cell.

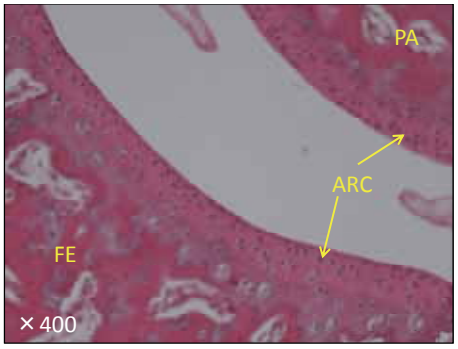

12. Knee joint in A (Female at 10Gy)

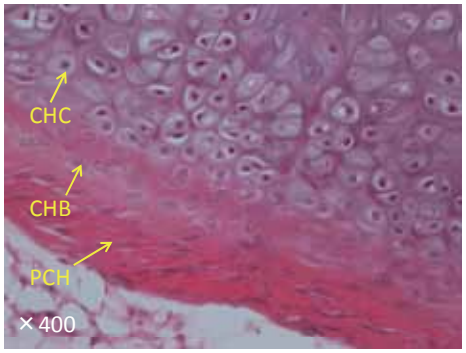

13. Costal cartilage in A (Female at 10Gy)

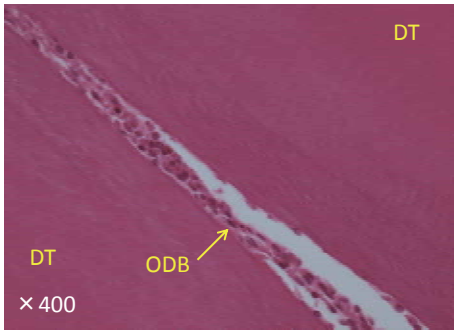

14. Dental pulp in C (Female at 10Gy)

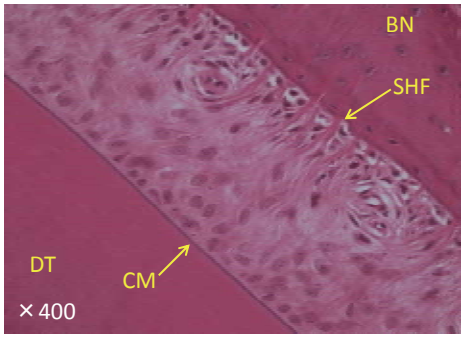

15. Periodontal memb. in C (Female at 10Gy)

Figs. 12-15. Sections of knee joint, costal cartilage, and incisor tooth. H&E staining. Magnification 400×. ARC, articular cartilage; BN, bone; CHB, chondroblast; CHC, chondrocyte; CM, cementum; DT, dentin; FE, femur; OB, osteoblast; ODB, odontoblast; PA, patella; PCH, perichondrium; SHF, Sharpey's fiber.

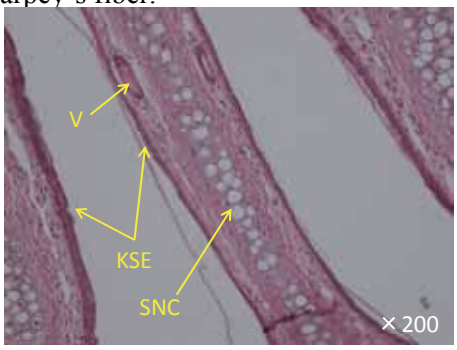

16. Nasal septum in A (Female at 10Gy)

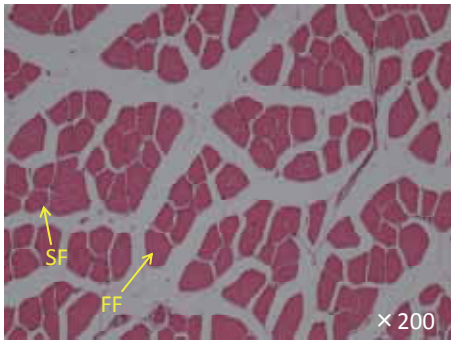

17. Gastrocnemius in A (Male at 10Gy)

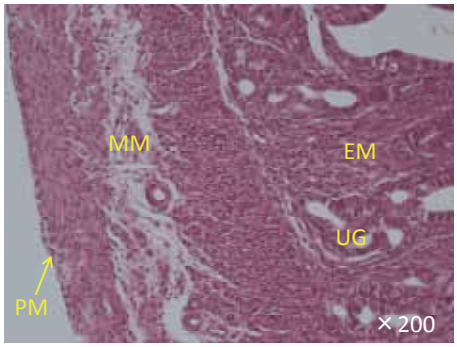

18. Uterine in A (Female at 10Gy)

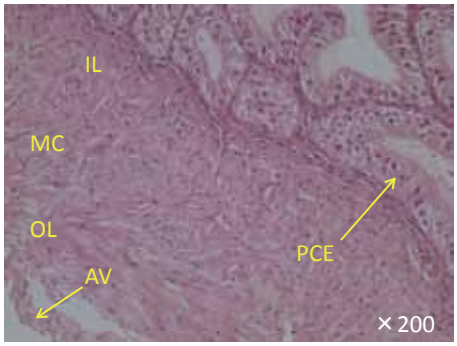

19. Ductus deferens in C (Male at 10Gy)

Figs. 16-19. Sections of nasal septum, gastrocnemius, uterus, and ductus deferens. H&E staining. Magnification 200×. AV, adventitia; EM, endometrium; FF, fast fiber; IL, inner longitudinal layer; KSE, keratinized stratified squamous epithelium; MC, middle circular layer; MM, myometrium; OL, uter longitudinal layer; PCE, pseudostratified ciliated epithelium; PM, perimetrium; SF, slow fiber; SNC, septal nasal cartilage; UG, uterine gland; V, vein or cavernous plexus.

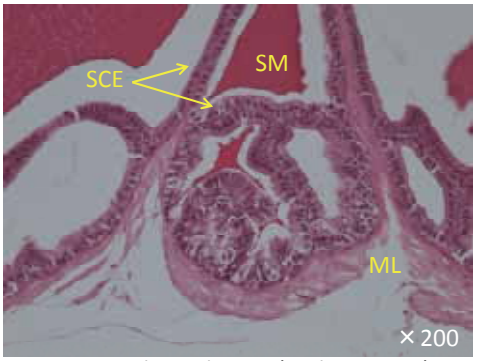

20. Seminal vesicle in A (Male at 10Gy)

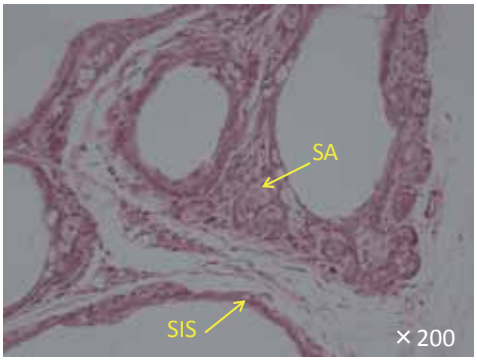

21. Preputial gland in A (Male at 10Gy)

22. Spongy urethra in A (Male at 10Gy)

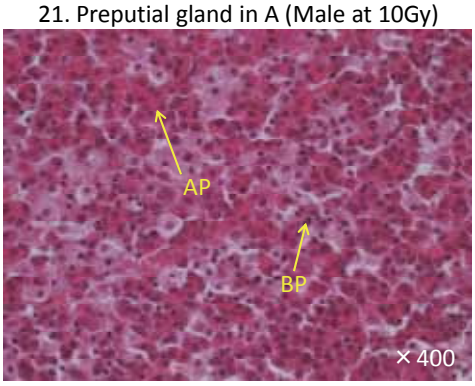

23. Pars anterior in C (Male at 10Gy)

Figs. 20–23. Sections of seminal vesicle, preputial gland, spongy urethra, and hypophysis. H&E staining. Magnifications 200× and 400×. AP, acidophil; BP, basophil; ML, muscle layer; SCE, simple columnar or cuboid epithelium; SA, sebaceous gland; SIS, simple squamous epithelium; SM, secretion material; TA, tunica albuginea; TRE, transitional epithelium.

*Corresponding to: Shoji Chiba, Professor, Hirosaki University Graduate School of Health Sciences, 66-1, Hon-cho, Hirosaki, 036-8564, Japan
E-mail: sh-chiba@cc.hirosaki-u.ac.jp

Indoor radon concentration at temporary houses in Fukushima Prefecture

Masahiro Hosoda[1], Shinji Tokonami[2], Atsuyuki Sorimachi[3], Yasutaka Omori[3], Tetsuo Ishikawa[3]

[1] Department of Radiological Life Sciences, Division of Medical Life Sciences, Hirosaki University, Graduate School of Health Sciences, Hirosaki, Japan
[2] Department of Radiation Physics, Hirosaki University, Institute of Radiation Emergency Medicine, Hirosaki, Japan
[3] Department of Radiation Physics and chemistry, Fukushima Medical University, 1 Hikarigaoka, Fukushima, 960-1295

Abstract. A number of evacuees from Namie Town continue to live in temporary housing. In the present study, the concentration of radon, which is a risk factor for lung cancer, was measured at temporary housing facilities in Fukushima Prefecture in order to estimate the annual internal exposure dose. A passive radon-thoron monitor using a solid-state track detector (CR-39) was used to evaluate the average radon concentration, and a pulse-type ionization chamber was used to evaluate the daily variation in radon concentration. Radon concentration was measured during the period from October 2012 to January 2013. The daily variation in radon concentration at Tsushima clinic exhibited the general pattern that has been reported in numerous studies. The average radon concentrations at temporary houses, apartments, and detached houses were 5, 7, and 9 Bq/m^3, respectively. Assuming the residents lived in these facilities for one year, the annual effective doses were evaluated to be 0.17, 0.21, and 0.29 mSv, respectively.

Key Words: radon, temporary house, Fukushima, effective dose

Introduction

A number of residents of Namie Town were evacuated to other locations, such as Fukushima City and Nihonmatsu City, as a result of the TEPCO Fukushima Daiichi Nuclear Power Station accident (Fig. 1), and a number of the evacuees are still living in temporary housing. Whole body count examinations to estimate internal exposure to radiocesium have been carried out by Fukushima Prefecture and Namie Town [1]. Many institutions measure radiocesium contamination of food using high-purity germanium detectors [2]. External dose estimations for children and pregnant woman have been carried out using glass dosimeters. The goal of these examinations was to estimate the effect of artificial radionuclides released from the reactor building. Thus, the effective dose by natural radionuclides was not considered in these examinations. Recently, the WHO proposed a

Fig.1 Map of Fukushima Prefecture. Several residents of Namie Town were evacuated to other locations.

reference level for indoor radon gas ranging from 100 to 300 Bq/m^3; radon inhalation is believed to increase the risk of lung cancer after tobacco smoking [3]. In the present study, the indoor radon concentration was measured at temporary housing

facilities in Fukushima Prefecture in order to estimate the annual internal exposure dose.

Materials and Methods

Measurement of indoor radon concentration using a passive method

A passive radon and thoron discriminative monitor (RADUET) using a solid-state track detector (CR-39) was used to evaluate the average radon concentration (Fig. 2) [4]. Since higher indoor radon concentrations have been observed in winter, the monitor was placed in 50 houses in Fukushima City, Nihonmatsu City, and Motomiya Town during the period from October 2012 to January 2013. A total of 25 houses were temporary facilities, including Tsushima Clinic, 14 were apartments, and 11 were detached houses.

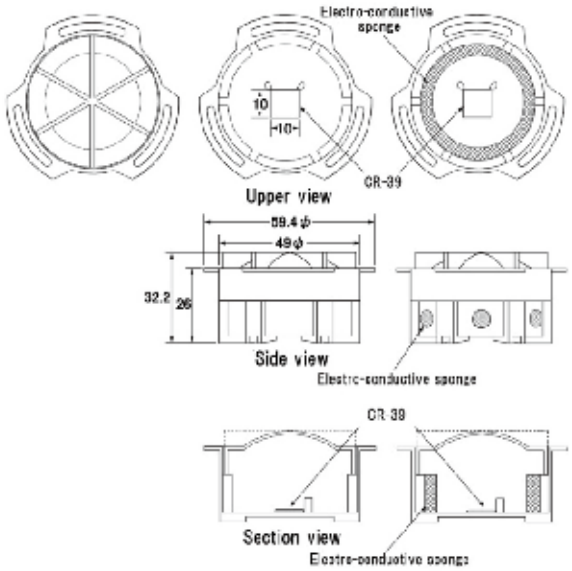

Fig.2 Outline of the passive type radon and thoron discriminative detector (RADUET) [4].

Measurement of indoor radon concentration using an active method

A pulse-type ionization chamber (AlphaGUARD) was used to evaluate the daily variation in radon concentration. AlphaGUARD was placed on the desk in Tsushima Clinic. The radon concentration was measured during the period from October 2012 to January 2013. The diffusion measurement mode was used with a time interval of 60 minutes. AlphaGUARD was calibrated in the radon calibration chamber at the National Institute of Radiological Sciences (NIRS), Japan (Fig. 3). The reference value of radon concentration in radon chamber at NIRS is based on the measurement value by standard ionization chamber which was calibrated at Physikalish Technische Bundesanstalt (PTB), Germany. The temperature and relative humidity in the radon calibration chamber can be controlled in the range 5-30°C with an error of 0.5°C, and 30-90% with an error of 3%, respectively [5, 6]. The calibration conditions for AlphaGUARD in the radon calibration chamber at NIRS were as follows. The average radon concentration, temperature, and relative humidity were 9,460 Bq/m^3, 21.0°C and 59.9%, respectively. The calibration factor for radon concentration was evaluated to be 0.995. The background concentration of AlphaGUARD was estimated using nitrogen gas and was determined to be 4.7 Bq/m^3.

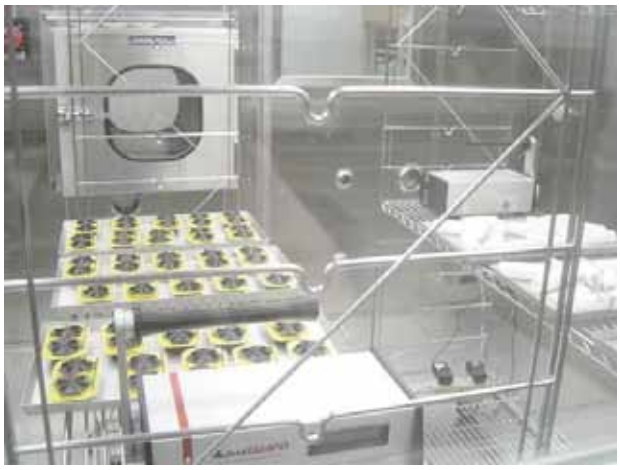

Fig.3 Calibration of AlphaGUARD in a radon chamber at NIRS.

Results and Discussion

The daily variation in radon concentration obtained using AlphaGUARD in the clinic is shown in Fig. 4, and it exhibits the general pattern reported in numerous studies [7]. The average radon concentrations ± the standard deviation obtained by RADUET at temporary housing facilities, apartments, and detached houses were 5 ± 3, 7 ± 3, and 9 ± 8 Bq/m^3, respectively. The difference in indoor radon concentration depending on the type of housing was not statistically significant. Annual effective doses were evaluated using the following equation which was reported by UNSCEAR [8]:

$$E = Q \cdot F \cdot T \cdot K \qquad (1)$$

Where, Q is the radon concentration (Bq/m^3), F is an equilibrium factor (indoors: 0.4, outdoors: 0.6), K is the dose coefficient (9×10^{-6} mSv/Bq h m^{-3}), and T is the occupancy factor. Assuming that residents lived in these houses for 1 year, the annual effective radiation dose due to indoor radon varied from ND to 0.9 mSv/y. Moreover, the average effective dose for each type of house was 0.17, 0.21 and 0.29 mSv/y, respectively. These are lower than the Japanese average, which was reported to be 0.45 mSv/y [9].

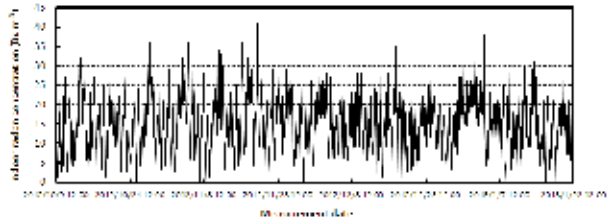

Fig. 4 Results of continuous measurement of indoor radon concentration using the AlphaGUARD.

References

[1] Hosoda M, Tokonami S, Akiba S, Kurihara O, Sorimachi A, *et al*. (2013) Estimation of internal exposure of the thyroid to ^{131}I on the basis of ^{134}Cs accumulated in the body among evacuees of the Fukushima Daiichi Nuclear Power Station accident. *Environ. Int.* **61**: 73-76.

[2] Harada K, Fujii Y, Adachi A, Tsukidate A, Asai F, *et al*. (2013) Dietary intake of radiocesium in adult residents in Fukushima Prefecture and neighboring regions after the Fukushima Nuclear Power Plant accident: 24-h food-duplicate survey in December 2011. *Environ. Sci. Technol*. **47(6)**: 2520-2526.

[3] World Health Organization. WHO Handbook on Indoor Radon - A Public Health Perspective-edited by Hajo Z and Ferid S (2009) http://whqlibdoc.who.int/publications/2009/9789241547673_eng.pdf

[4] Tokonami S, Takahashi H, Kobayashi Y, Zhuo W, Hulber E. (2005) Up-to-date radon-thoron discriminative detector for a large scale survey. *Rev. Sci. Instrum*. **76**: 113505.

[5] Ichitsubo H, Yamada Y, Shimo M, Koizumi A. (2004) Development of a radon-aerosol chamber at NIRS-general design and aerosol performance. *J. Aerosol Sci*. **35**: 217-232.

[6] Tokonami S. (2009) Thoron in the environment and its related issues. *Indian J. Phys*. **83(6)**: 777-785.

[7] Sorimachi A, Kranrod C, Tokonami S, Ishikawa T, Hosoda M, *et al*. (2009) Anomalously high radon concentrations in a dwelling in Okinawa, Japan. *RADIOISOTOPES* 58:807-813.

[8] United Nations Scientific Committee on the Effects of Atomic Radiation. (2000) UNSCEAR 2000 Report to the general assembly with scientific annexes. United Nations.

[9] Sanada T, Fujimoto K, Miyano K, Doi M, Tokonami S, *et al*. (1999) Measurement of nationwide indoor Rn concentration in Japan. *J. Environ. Radioact*. **45**: 129-137.

Acknowledgments

The authors would like to thank Dr. Shunji Sekine and Mr. Norio Konno, at the Tsushima Clinic, for their kind assistance in carrying out this study.

Cytotoxic effects of hyper-radiation sensitivity with low-dose fractionation exposure

Yui Inoue, Shingo Terashima*, and Yoichiro Hosokawa

Department of Radiological Technology, School of Health Sciences, Hirosaki University

Abstract. Reports to date suggest that prolonged periods between radiation exposures might have a negative biological effect on cancer cells in both intensity-modulated radiation therapy and stereotactic radiation therapy. However, more effective cell death, called hyper-radiation sensitivity (HRS), has been reported at low doses of radiation (<1 Gy). In this study, we examined the cytotoxic effect of low-dose fractionation exposures administered at short time intervals. We evaluated the cell survival rate of human lung A549 cells and Chinese hamster V79 cells using colony assays. First, we exposed these cells to a radiation dose rate of 2.0 Gy/min. Total doses of 2, 4, and 8 Gy were given by fractionated radiation in unit doses of 0.25, 0.5, 1.0, and 2.0 Gy at 10-sec intervals. Next, we exposed cells to 2 Gy of X-rays at dose rates of 1.0, 1.5, and 2.0 Gy/min at 1-min intervals using the same unit doses as above. An increased cytotoxic effect was observed with low-dose fractionation exposure compared to a single exposure. Cell survival rates with fractionation exposure using a unit dose of 0.25 Gy were remarkably lower compared with a single exposure delivering the same dose. When the dose rates were lower (1.0 and 1.5 Gy/min), the cytotoxic effect decreased compared to exposure to a dose rate of 2.0 Gy/min. These results indicate that more effective cell death is induced with low-dose fractionation exposures for a given dose due to the HRS phenomenon, and suggest that application of HRS will improve the therapeutic effects of radiation therapies.

Key Words: hyper-radiation sensitivity, radiation therapy, low-dose fractionation exposure

* Corresponding to: Shingo Terashima, Research Associate, Hirosaki University, 66-1, Hon-cho, Hirosaki, 036-8564, Japan. E-mail: s-tera@cc.hirosaki-u.ac.jp

Introduction

Current evidence suggests that prolonged intervals between radiation treatments might have a negative biological effect on cancer cells in intensity-modulated and stereotactic radiation therapy. However, the biological effect of fractionation exposure, in which the intervals between radiation treatments are short, remains unclear, and conflicting data (decreased or increased surviving fraction) have been reported. On the other hand, enhanced cell lethality, termed hyper-radiation sensitivity (HRS), has been reported at low doses of radiation (<1 Gy) (Figure 1) [1]. Fractionation exposure has typically been studied using intervals of several hours (for example, 0.5 Gy × 4 at 8 hour intervals) using HRS[2, 3]. We conducted this study to examine the effect of low-dose fractionation exposures with a short time interval for the purpose of clinical application.

Materials and Methods

Cell culture

Human lung A549 cells and Chinese hamster V79 lung cells were used. Cells were cultured in DMEM/Ham's F-12(A549) and Ham's F-12(V79) media supplemented with 10% fetal bovine serum and were maintained at 37°C with 95% air and 5% CO_2.

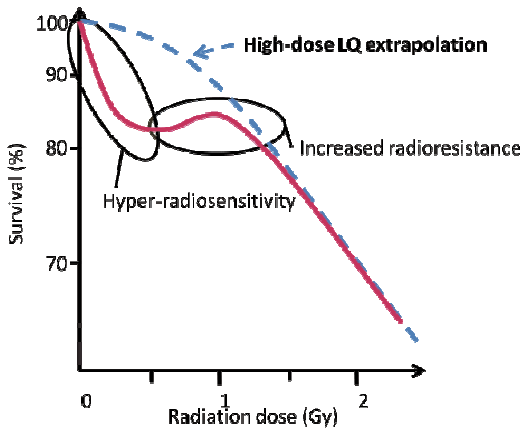

Figure 1. Schematic diagram showing hyper-radiosensitivity (HRS)

X-irradiation and irradiation schedule

X-irradiation was delivered using a MBR-1520R-3 X-ray machine (Hitachi Medico Technology, Tokyo, Japan) at 150kVp through a 0.5 mm Al and 0.1 mm Cu filter. First, cells were exposed to total doses of 2, 4 and 8 Gy by fractionated radiation in unit doses of 0.25, 0.5, 1.0 and 2.0 Gy at 10-sec intervals. Cells were then exposed to various dose rates as follows: total doses of 2 Gy were given by fractionated radiation in unit doses of 0.25, 0.5, 1.0 and 2.0 Gy at rates of 1.0, 1.5 and 2.0 Gy/min at 1 min intervals. Finally, cells were exposed for various time intervals to a total dose of 2 Gy given by fractionated radiation in unit doses of 0.25, 0.5, 1.0 and 2.0 Gy at a dose rate of 2.0 Gy/min at 10 sec, 1-min and 3-min intervals. An example radiation schedule is shown in Figure 2.

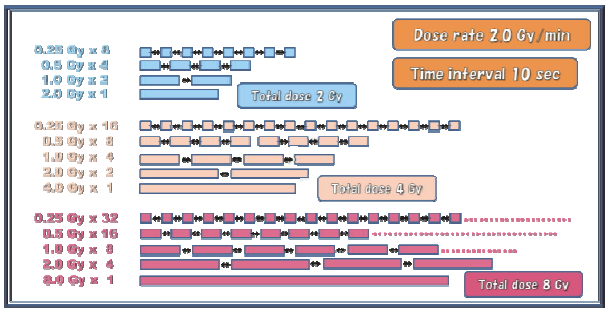

Figure 2. Schematic diagram of the radiation schedule. Cells were exposed to low-dose fractionation with various total doses.

Clonogenic assays

Briefly, both A549 and V79 cells were plated onto culture dishes and irradiated 6 hours later according to the above irradiation schedule. After incubation for 7–14 days, colonies were stained with Giemsa, and colonies containing more than 50 cells were counted.

Statistical analysis

Statistical comparisons were performed using the Tukey-Kramer test. All results are presented as the mean±SD from the results of at least three independent experiments.

Results

An increase in cytotoxicity was observed following low-dose fractionation exposure compared to single exposure. Significant cytotoxicity due to low-dose fractionation exposure (0.25 Gy×8) was observed in both A549 and V79 cells following low-dose fractionation exposure at varying total dose. Cytotoxicity was enhanced as the total dose increased, up to 8 Gy (Figure 3).

The results also suggested that cytotoxicity is influenced by the dose rate and time interval. At lower dose rates (1.0 and 1.5 Gy/min), cytotoxicity caused by low-dose fractionation decreased compared with exposure at 2.0 Gy/min (Figure 4). Significant cytotoxic effects were observed when both A549 and V79 cells were exposed to low-dose fractionation at 2.0 Gy/min. However, in A549 cells, no significant differences in cytotoxicity were observed between low-dose fractionation exposures (0.25 Gy×8) and single exposure at 1.0 Gy/min. Similarly, no significant differences in cytotoxicity were observed between low-dose fractionation exposures (0.25 Gy×8) and single exposure at 1.0 Gy/min and 1.5 Gy/min in V79 cells.

Significant cytotoxic effects were observed when A549 cells were exposed to low-dose fractionation (0.25 Gy×8) using 10-sec, 1-min and 3-min intervals, compared to a single exposure. On the other hand, the cytotoxic effect was decreased when V79 cells were exposed to low-dose fractionation (0.25 Gy×8) at 3-min intervals, compared to shorter time intervals (10-sec and 1-min) (Figure 5).

Conclusion

This study showed that cytotoxicity in both human and Chinese hamster lung cells arises from short time interval, low-dose fractionation exposure involving HRS. Furthermore, this cytotoxicity decreased at lower dose rates. Our results indicate that utilization of the HRS phenomenon will likely improve the therapeutic effects of radiation therapy.

References

[1] Marples, Brian, and Spencer J. Collis. Low-dose hyper-radiosensitivity: past, present, and future. International Journal of Radiation Oncology* Biology* Physics. 70(5):1310-1318(2008).

[2] Dey, Swatee, et al. Low-dose fractionated radiation potentiates the effects of Paclitaxel in wild-type and mutant p53 head and neck tumor cell lines. Clinical cancer research. 9(4):1557-1565(2003).

[3] C. Short, J. Kelly, CR Mayes, M. Woodcock, MC Joiner, S. Low-dose hypersensitivity after fractionated low-dose irradiation in vitro. International journal of radiation biology. 77(6):655-664(2001).

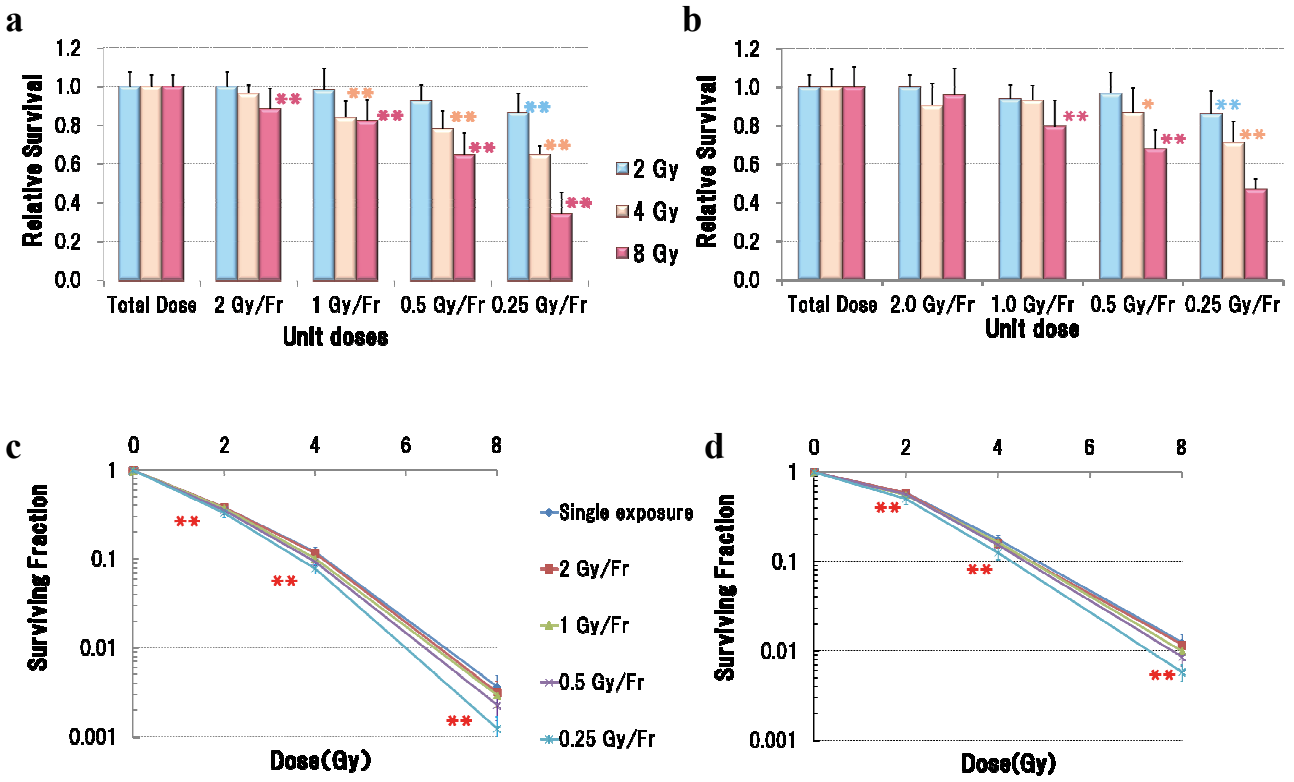

Figure 3. Clonogenic survival and cell survival curves for A549 (a, c) and V79 (b, d) cells after exposure to low-dose fractionation with various total doses. Total doses of 2, 4, and 8 Gy were given by fractionated radiation in unit doses of 0.25, 0.5, 1.0 and 2.0 Gy at 2.0 Gy/min at 10-sec intervals.
*p < 0.05, **p < 0.01 vs. single exposure

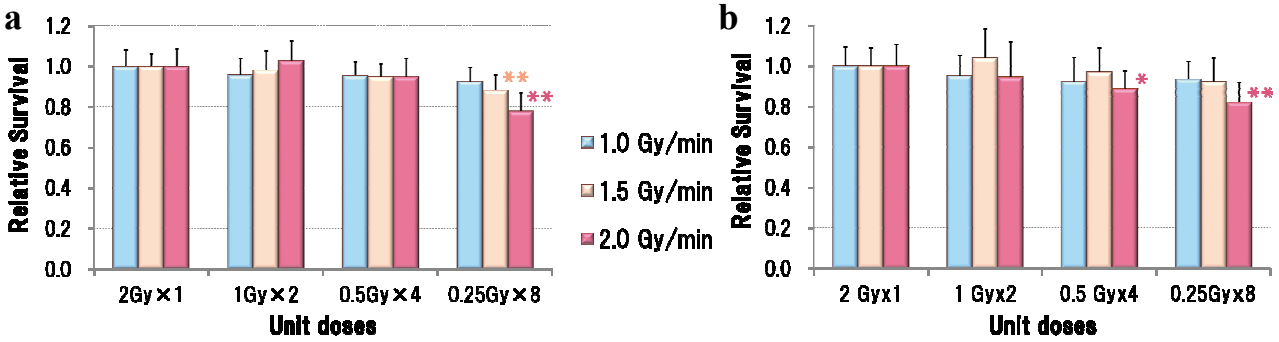

Figure 4. Clonogenic survival of A549 (a) and V79 (b) cells after exposure to low-dose fractionation with various dose rates. Total doses of 2 Gy were given by fractionated radiation in unit doses of 0.25, 0.5, 1.0 and 2.0 Gy at 1.0, 1.5, and 2.0 Gy/min at 1-min intervals.
*p < 0.05, **p < 0.01 vs. single exposure

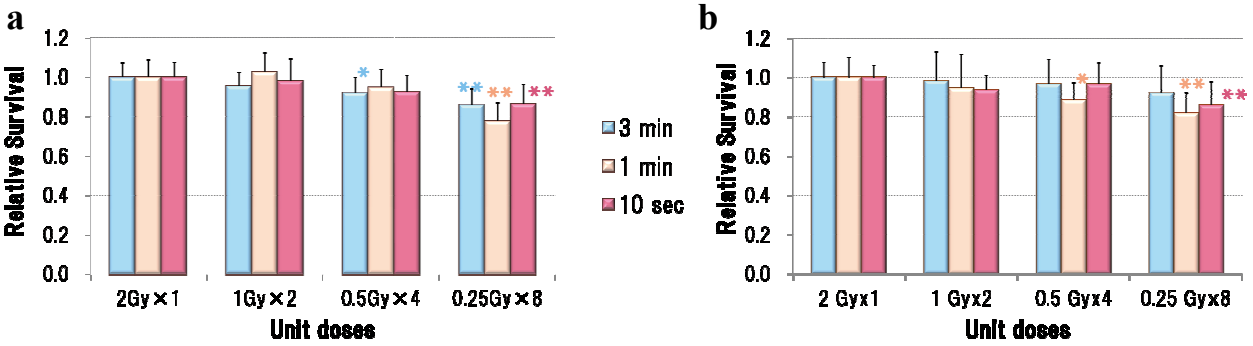

Figure 5. Clonogenic survival of A549 (a) and V79 (b) cells after exposure to low-dose fractionation with various time intervals. Total doses of 2 Gy were given by fractionated radiation in unit doses of 0.25, 0.5, 1.0 and 2.0 Gy at 2.0 Gy/min at intervals of 10-sec, 1-min, and 3-min.

Effect of X-ray dose level on activities of glutathione-related antioxidant enzymes and glutathione concentration in rats

Takashi Ishikawa[1*], Shinya Kudo[2], Yuya Sato[2], Kyoko Nakano[1], Naoki Nanashima[1, 3] and Toshiya Nakamura[1, 3]

[1] Department of Biomedical Sciences, Division of Medical Life Sciences, Hirosaki University Graduate School of Health Sciences, Hirosaki, Japan
[2] Department of Medical Technology, Hirosaki University School of Health Sciences, Hirosaki, Japan
[3] Research Center for Biomedical Sciences, Hirosaki University Graduate School of Health Sciences, Hirosaki, Japan

Abstract. It has been reported that the glutathione (GSH)-related antioxidant defence system is modulated in irradiated tissue and serum. To clarify the effect of radiation dose on the system, we investigated the effect of X-ray dose level on GSH-related enzyme activities, as well as on GSH concentration, in rats. Male rats were exposed to a single X-ray irradiation treatment at one of several doses up to 7 Gy and the liver, kidney, testis and small intestine were exenterated 24 h after irradiation. GSH concentration and the activities of glutathione S-transferees (GST), glutathione reductive (GR), and glutathione peroxidase of each tissue were measured; the activities of these enzymes were also assayed in serum and urine. GR activity was up-regulated in the liver and testis, and GSH concentration was increased in the small intestine. GST activity was down-regulated in the kidney; however, these changes did not occur in a dose-dependent manner. Serum enzyme activities were not affected, whereas most urinary enzyme activities increased in a dose-dependent manner up to 2 Gy. These results suggest that urinary GSH-related enzyme activities could be applicable for dose assessment in radiation emergency situations.

Key Words: GSH concentration, GSH-related enzyme activity, X-ray dose-level, rat

1. Introduction

The glutathione (GSH)-related antioxidant defence system are involved in the metabolism and detoxification of cytotoxic and carcinogenic compounds as well as reactive oxygen species (ROS) [1, 2]. The system consists of GSH, glutathione S-transferase (GST), glutathione reductase (GR) and glutathione peroxidase (GSH-Px). ROS can be detoxified by GSH, GST P1-1 form and GSH-Px. Superoxide dismutase (SOD) and catalase (CAT), which are not components of the defence system, also inactivate ROS. GSH can either act as a substrate in the cytosolic GSH redox cycle or directly inactivate ROS such as superoxide and hydroxyl radicals [3]. Furthermore, lipid hydroperoxide, which is a lipid peroxidation product, can be reduced by GSH-Px and several GST isozymes [4-6]. GR functions to convert oxidized glutathione to the reduced form, GSH. It has been reported that the defence system is modulated in irradiated tissue and serum within 24 h after irradiation [7–9]; however, the effect of radiation dose on the system remains unclear. Therefore, we investigated the effect of X-ray dose level on GSH-related enzyme activity, as well as on the GSH concentration, in rats.

2. Materials and method

[*] Correspondence to: Takashi Ishikawa, Lecturer, Hirosaki University Graduate School of Health Sciences, 66-1, Hon-cho, Hirosaki 036-8564, Japan
E-mail: ti3054@cc.hirosaki-u.ac.jp

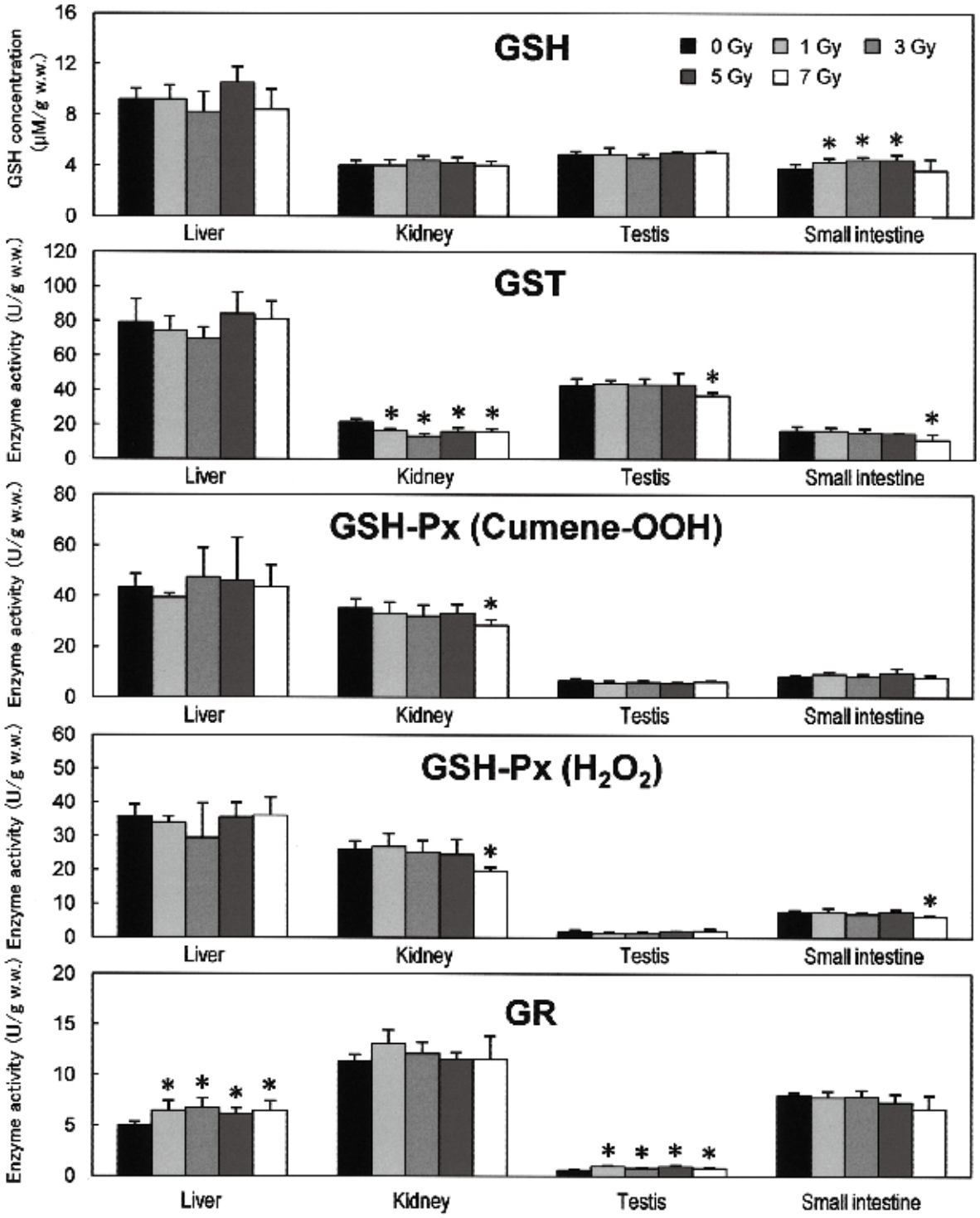

Figure 1. Effect of radiation dose level on GSH concentration and GSH-related enzyme activities in the liver, kidney, testis and small intestine. All values are expressed as mean ± SD of six animals.
* Significant ($p < 0.05$) when compared with the control (0 Gy) group.

2.1 X-ray irradiation

Six-week old male Sprague-Dawley rats were exposed to a single X-ray irradiation treatment at one of several doses (1, 3, 5 and 7 Gy) under the following conditions: 150 kV, 20 mA, 1.0-mm aluminium filter, 1.6 Gy/min. The control rats were

subjected to a sham irradiation. Each rat was then returned to its individual metabolic cage. The urine of each rat was collected in a holder attached to the cage for 24 h post irradiation.

2.2 Sample preparation

The liver, kidney, testis, and small intestine were exenterated, and serum was separated from withdrawn blood 24 h after irradiation. Each tissue was homogenized with 45 mM Tris-HCl buffer (pH 7.4) containing 170 mM KCl, 4 mM EDTA and 5 mM DTT for enzyme activity determination, and the cytosol fraction was obtained by ultracentrifugation. For GSH concentration determination, 5.5% trichloroacetic acid was used as the homogenizing medium.

2.3 Enzyme activity and creatinine assays

GSH concentration and the activity of GST, GR, and GSH-Px of each cytosol fraction were measured at 25°C. GST activity was assayed using 1-chloro-2,4-dinitrobenzene as a substrate. GSH-Px activity was measured with two substrates, hydrogen peroxide (H_2O_2) and cumene hydroperoxide (cumene-OOH). Cumene-OOH was used as a lipid hydroperoxide. These GSH-related enzyme activities were also measured in serum and urine. In addition, urinary creatinine concentration was determined and used to correct the enzyme activities to reflect their urinary concentrations.

3. Results

3.1 Effect of X-ray irradiation on tissue GSH concentration and GSH-related enzyme activities

In the tissues examined, GSH concentration in the small intestine increased following irradiation at up to 5 Gy, and GR activity was up-regulated in the liver and testis at all dose levels (Figure 1). However, GST activity was down-regulated at all dose levels in the kidney, and was decreased in the testis and small intestine following irradiation at 7 Gy. GSH-Px activity towards H_2O_2 was decreased in the kidney and small intestine, and the activity towards cumene-OOH was decreased in the kidney

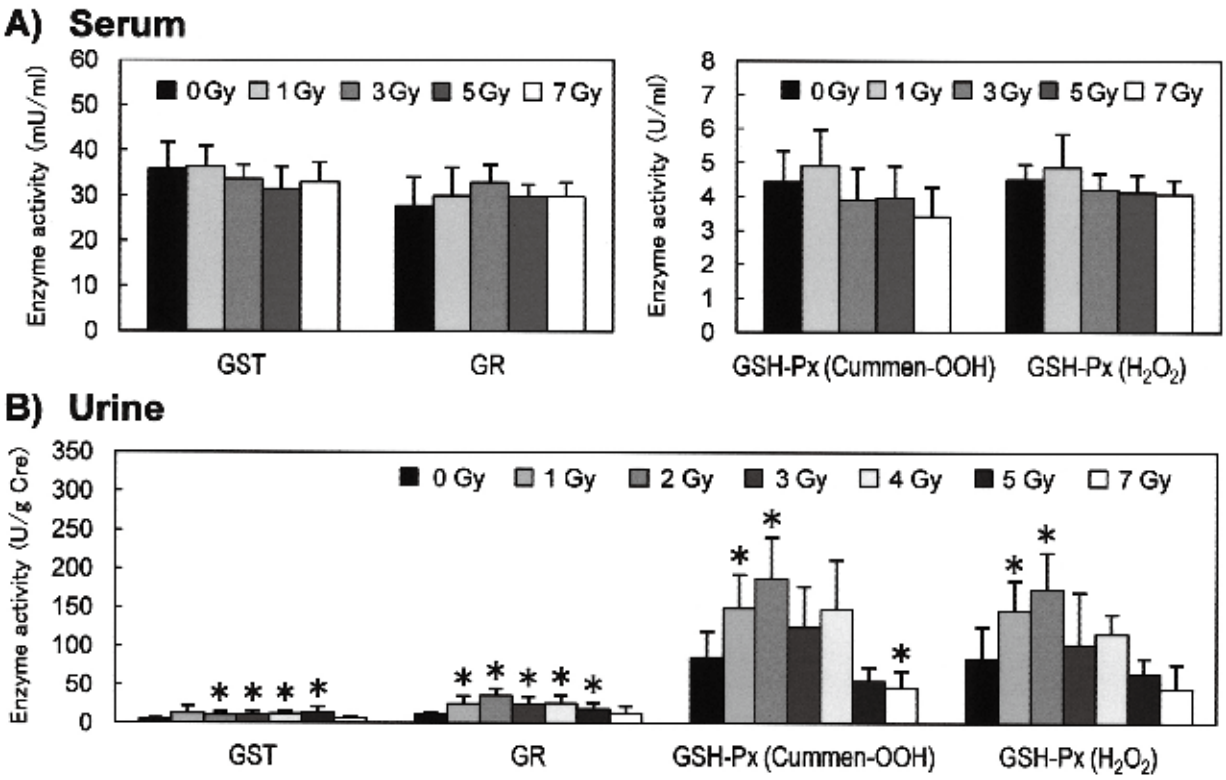

Figure 2. Effect of radiation dose level on GSH-related enzyme activities in serum (A) and urine (B). All values are expressed as mean ± SD of six animals. Value of each urinary enzyme activity is described as units per gram of creatinine (U/g Cr).
* Significant ($p < 0.05$) when compared with the control (0 Gy) group.

following exposure to 7 Gy. Thus, kidney GST activity is highly sensitive to X-ray exposure.

3.2 Effect of X-ray irradiation on serum and urinary GSH-related enzyme activities

No GSH-related enzyme activities in serum were affected by X-ray irradiation (Figure 2A), whereas all urinary enzyme activities were increased in urine (Figure 2B). In particular, GST activity was uniformly increased at doses of between 2 and 5 Gy, but returned to the control level at 7 Gy. In contrast, the activities of the other GSH-related enzymes increased in a dose-dependent manner up to 2 Gy and fell gradually to the control level at 5 or 7 Gy.

4. Discussion

The experimental results suggest that the effects of X-ray irradiation on GSH concentration and GSH related serum enzymes are dose-independent and tissue-specific, but that X-ray irradiation has a dose-dependent effect on urinary enzyme activities at low dose levels. However, other detoxification enzymes help attenuate oxidative stress. Accordingly, the effect of radiation on their activities, in particular SOD and CAT, should be investigated in the future.

In this study we found that, except for GST activity, other urinary enzyme activities increased in a dose-dependent manner up to 2 Gy, suggesting the potential utility of urinary enzymes as biomarkers of external radiation exposure. However, no single enzyme activity appears to reveal whether the exposed dose level is less than 2 Gy or more than 2 Gy. Recently, we found that rat urinary N-acetyl-beta-D-glucosaminidase (NAG) activity increases significantly between 3 to 7 Gy compared with the control before irradiation (data not shown). In the future, investigations combining other assays such as NAG activity measurements may clarify the suitability of GSH-related enzyme activities for assessing doses in radiation emergency situations.

5. Acknowledgement

This work was supported by a grant from the Co-medical Education Program in Radiation Emergency Medicine from the Ministry of Education, Culture, Sport, Science and Technology, Japan, and by a grant from Hirosaki University Institutional Research.

References

[1] Beckett GJ and Hayes JD. Glutathione S-transferases: Biomedical applications. *Adv Clin Chem*. 30: 281-380 (1993).

[2] Hayes JD and Pulford DJ. The glutathione S-transferase supergene family: Regulation of GST and the contribution of the isoenzymes to cancer chemoprotection and drug resistance. *Crit Rev Biochem Mol Biol*. 30: 445-600 (1995).

[3] Meister A. Glutathione metabolism and its selective modification. J Biol Chem. 263: 17205-17208 (1988).

[4] Kitahara A, Yamazaki T, Ishikawa T, Camba EA and Sato K. Changes in activities of glutathione peroxidase and glutathione reductase during chemical hepatocarcinogenesis in the rat. *Gann* 74: 649-655 (1983).

[5] Sato K, Satoh K, Tsuchida S, Hatayama I, Shen H, Yokoyama Y, Yamada Y and Tamai K. Specific expression of glutathione S-transferase Pi form in (pre) neoplastic tissues: Their properties and functions. *Tohoku J Exp Med*. 168: 97-103 (1992).

[6] Knapen MF, Zusterzeel PL, Peters WH, Steegers EA. Glutathione and glutathione-related enzymes in reproduction. A review. *Eur J Obstet Gynecol Reprod Biol*. 82: 171-184 (1999).

[7] Rao BN, Rao BS, Aithal BK, Kumar MR. Radiomodifying and anticlastogenic effect of zingerone on swiss albino mice exposed to whole body gamma radiation. *Mutat Res*. 677: 33-41 (2009).

[8] Sener G, Jahovic N, Tosun O, Atasoy BM, Yeğen BC. Melatonin ameliorates ionizing radiation-induced oxidative organ damage in rats. *Life Sci*. 74: 563-572 (2003).

[9] Navarro J, Obrador E, Pellicer JA, Aseni M, Viña J and Estrela JM. Blood glutathione as an index of radiation-induced oxidative stress in mice and human. *Free Radic Biol Med*. 22: 1203-1209 (1997).

Attitudes of public health nurses in relation to radiation screening after the Fukushima Daiichi nuclear power plant accident

Chiaki Kitamiya*

Department of Health Promotion, Division of Health Sciences, Graduate School of Health Sciences, Hirosaki, Japan

Abstract. The movement of residents from Fukushima Prefecture to other prefectures started after the accident at the Fukushima Daiichi nuclear power plant. Ibaraki Prefecture screened these evacuees for radioactive substances on March 15, 2011 at three public health centers. Staff members of these health centers were also involved in the screening, and the public health nurses (PHNs) who worked for these centers were surveyed. Their attitude concerning their work as PHNs was clarified at that time.

The PHNs who participated in this research study comprised two women. Personal Attitude Construct analysis was used as the research technique. The analysis procedure was as follows: 1) Presentation of a sentence for association; 2) the sentence was freely associated; 3) importance was applied to the sentence; 4) the degrees of similarity of the associations were determined; 5) cluster analysis was performed; and 6) the image of the cluster was interpreted. This study was approved by the Committee of Medical Ethics of Hirosaki University Graduate School of Medicine in Hirosaki, Japan.

One PHN perceived three clusters as follows: Cluster 1, activities conducted within the scope of what public health nurses can do; Cluster 2, the screening environment was worked out through trial and error; and Cluster 3, after the survey, the accident victims were sent to the evacuation site. The other PHN perceived two clusters: Cluster 1, first of all, an accident victim's uneasiness was lessened by caring; and Cluster 2, the radiation screening was associated with anxiety.

Public health nurses tried as much as possible to allay the uneasiness of the evacuees during radiation screening. In addition, they were also introducing the evacuees to the evacuation site. They devised and executed the screening in an inadequate environment; however, they believed it went well and they accepted the difficulties as part of the necessary trial and error approach.

Key Words: radiation screening, PHN, PAC analysis, caring for nuclear accident victims

*Correspondence to: Chiaki Kitamiya, Associate Professor
Hirosaki University, 1-66, Hon-cho, Hirosaki 036-8564, Japan
TEL:(+81) (0)172-39-5945 FAX: (+81) (0)172-39-5945
E-mail: chiaki@cc.hirosaki-u.ac.jp

Introduction

The movement of residents from Fukushima Prefecture to other prefectures started after the accident at the Fukushima Daiichi nuclear power plant. Ibaraki Prefecture screened these evacuees for radioactive substances on March 15, 2011 at three public health centers. The staff members of the public health centers were involved in the screening. Ibaraki Prefecture had implemented the national protection training program in case of nuclear terrorism ahead of the Great East Japan Earthquake. In addition, the prefecture experienced a critical accident at JCO, Ltd. in 1999.

Purpose

The purpose of this study was to survey the public health nurses (PHNs) who worked for these three public health centers in Ibaraki Prefecture, and to clarify attitudes regarding their work as PHNs at that time.

Methods

The PHNs who participated in the research comprised two women. They were approximately 50 years of age and had considerable experience, including dealing with residents affected by the JCO accident.

Interviews with the PHNs were conducted one year after the Great East Japan Earthquake, which occurred on March 11, 2011. Personal Attitude Construct (PAC) analysis was used as the technique in this research study.

The analysis procedure was as follows: 1) A sentence was presented for association; 2) the sentence was freely associated; 3) importance was applied to the sentence; 4) the degrees of similarity of the associations were determined; 5) cluster analysis was performed; and 6) the image of the cluster was interpreted.
The stimulus for association was as follows.

Table 1. Public health nurse 1's clusters

Clusters	Importance	Association
Activities conducted within the scope of what public health nurses can do.	2	Allaying of uneasiness to exposure (caring for the evacuees' understanding at that time)
	7	Processing of clothes with a high dose of radiation (undressing for decontamination)
	5	The uneasiness of the person with high-dose exposure was lessened. Hospital referral (guide and adjustment)
	11	Allaying the uneasiness with respect to exposure (Radiation dosimetry was to be performed for evacuees from a 20-km radius; however, we performed radiation dosimetry for all evacuees. The public health nurse responded to the questions of the evacuee at the same time.)
	13	Dealing with the exposure of the evacuee and the shelter destination of the evacuee
	6	We responded to the various anxieties of the evacuees (easing plan).
	1	The possibility of exposure was confirmed.
The screening environment was prepared in a trial and error fashion.	3	Environmental considerations: Heating was provided; however, due to the low outdoor temperature, it was insufficient. Consequently, prompt screening was borne in mind.
	8	The needs of senior citizens and children were considered.
After the screening, we sent accident victims to the evacuation site.	10	Diseases of the evacuee were confirmed.
	12	We introduced the evacuation site to the evacuee (after setting up the evacuation site in the prefecture).
	4	When travel to shelter at a long distance was difficult due to sickness, the evacuation site was changed (acceptance of the evacuee was requested from the city).
	9	Concern about shelter and medical treatment of the evacuee in the future.

Table 2. Public health nurse 2's clusters

Clusters	Importance	Association
First of all, the accident victim's uneasiness was lessened by caring.	4	I wanted to speak to the evacuee politely.
	9	I wanted information to be conveyed (e.g., evacuation site information) to the evacuee.
	3	I wanted to speak with the evacuee to provide relief. I wanted to make the evacuee feel safe.
	10	When I think of the evacuee, I feel pain.
The radiation screening was associated with anxiety.	1	I wanted the opinion of a specialist.
	8	I wanted information about the accident.
	5	The survey was to be performed for evacuees in a 20-km radius from the nuclear power plant; however, I wanted to relieve the anxiety of all the evacuees.
	2	It is uncomfortable to know that there is no field commander.
	7	Site management should appropriately segregate the polluted area from clean areas.
	6	The effects of exposure on the body at different levels are poorly understood.

"Please answer with respect to your involvement in screening the evacuees from Fukushima. What do you think was important in the screening activity? What actions did you perform for the evacuees?"

The PHNs then freely described their associations. Next, the PHNs evaluated the importance of the described content. In addition, the degrees of similarity of the descriptions were evaluated on a scale of 1–10. A cluster analysis of these data was performed using statistical analysis software (HALWIN 7.3, CMIC Co., Ltd, Tokyo, Japan). The results of the cluster analysis were shown to the PHNs, and the PHNs subsequently decided on the classification of the clusters.

This study was approved by the Committee of Medical Ethics of Hirosaki University Graduate School of Medicine in Hirosaki, Japan. Verbal and written explanations of the ethical considerations were provided to the participants at the time of their interviews, and the study was started after written, informed consent was obtained from all participants.

Results and Discussion

One public health nurse perceived three clusters as follows: Cluster 1, activities conducted within the scope of what public health nurses can do; Cluster 2, the screening environment was worked out through trial and error; and Cluster 3, after the survey, the accident victims were sent to the evacuation site (Table 1). Cluster 1 was related to the public health nurse thinking of her role and work during the screening. Cluster 2 involved system development that considered people. Cluster 3 was related to the content of the activity that had been conducted to avoid embarrassing the evacuees.

The other public health nurse perceived two clusters: Cluster 1, first of all, an accident victim's uneasiness was lessened by caring; and Cluster 2, the radiation screening was associated with anxiety (Table 2). Cluster 1 was the attitude of the public health nurse who accepted the evacuee. Cluster 2 was seen as an unresolved problem that the PHN felt needed to be addressed.

Public health nurses tried as much as possible to allay the uneasiness of the evacuees during radiation screening. In addition, the PHNs were also introducing the evacuees to the evacuation site. The PHNs devised and executed the screening in an inadequate environment; however, they believed it went well, and they accepted the difficulties as part of the necessary trial and error approach.

Acknowledgments

The cooperation of Mr. Hitoshi Araki of the Ibaraki Hitachinaka Health Center in this study is deeply appreciated. The authors wish to express their gratitude to the public health nurses who participated in the interviews.

The influence of high-dose radiation on rat skin and muscle: Developing an animal model of local radiation damage to the hind limbs (2nd report)

Shuhei Koeda [1*], Hirokazu Narita[1], Koichi Ito[2], Kyoko Ito[2], Haruhiko Yoshioka[3] and Hitoshi Tsushima[1]

[1] Department of Development and Aging, Division of Health Sciences, and Departments of [2]Biomedical Sciences and [3]Pathogenic Analysis, Division of Medical Life Sciences, Hirosaki University Graduate School of Health Sciences, Hirosaki, Japan

Abstract. The purpose of this preliminary study was to develop an animal model of local radiation damage of the hind limbs. Fourteen male Wistar rats were randomly divided into the following groups: a control group (Con-G), a 30-Gy X-ray irradiation group (30 Gy-G), and a 50-Gy X-ray irradiation group (50 Gy-G). Only the hind limbs of the rats were irradiated. The state of the hind limbs, the weight of each rat, and the spontaneous activity and range-of-motion (ROM) of dorsiflexion of the ankle joints were measured for 6 weeks after irradiation. The soleus muscles of each rat were then extracted and their wet weights measured. The 30 and 50 Gy-G showed hair loss, tumours, and effusions two weeks after irradiation. The weights in the 30 and 50 Gy-G were stable for three weeks after irradiation. The spontaneous activity and the ROM of the 30 and 50 Gy-G decreased for three weeks after irradiation, then increased in the 30 Gy-G. The wet weights of the soleus muscle were lower in the 30 and 50 Gy-G than in the Con-G. The clinical condition of the 50 Gy-G was observed and found to remain stable throughout the study period. Therefore, a radiation dose of at least 50 Gy is required to develop an animal model of local radiation damage.

Key Words: Radiation damage, skin, muscle, animal model, rehabilitation

[*] Corresponding to: Shuhei Koeda, Assistant Professor, Hirosaki University, 66-1, Hon-cho, Hirosaki, 036-8564, Japan.
E-mail: ot_koeda@cc.hirosaki-u.ac.jp

Introduction

We have reviewed the literature dealing with the rehabilitation of patients undergoing high dose radiation treatments to better understand the role of rehabilitation in radiation emergency medicine [1, 2]. It is clear that rehabilitation, including early ambulation and respiratory care, is very important for recovery of patients exposed to radiation. In particular, the efficacy of rehabilitation exercises for easing muscle and skin injuries was emphasized. However, there are very few reports dealing with either rehabilitation of patients treated with high-dose radiation or fundamental research on high-dose radiation exposure. Therefore, it is unclear how rehabilitation exercises can help address muscle and skin disorder caused by high-dose radiation.

The purpose of this study was to determine the effects of rehabilitation exercise on high-dose radiation injuries. We are in the process of developing an animal model of local radiation damage of the hind limbs. This paper reports the progress and problems encountered in developing an appropriate animal model.

Materials and Methods

Subjects comprised 14 male, 4-week-old Wistar rats (Clea, Tokyo, Japan). All rats were given ad libitum access to standard laboratory diet and water under a 12-h light/dark cycle. The rats were randomly divided into the following groups: a control group (Con-G, n=3), a 30-Gy X-ray irradiation group (30 Gy-G, n=5), and a 50-Gy X-ray irradiation group (50 Gy-G, n=6). The rats were accustomed to a Wheel Meter (Lafayette Instruments, Lafayette, IN) that was used to measure their spontaneous activity at the age of 9 weeks.

At 9 weeks of age, the rats were anesthetized with an intraperitoneal injection of sodium pentobarbitone (40 mg/kg), and their hind limbs (except toes and metatarsal regions) were irradiated using a fixation device developed in our laboratory. The rest of the body, including the toes and metatarsal regions, were completely shielded with 4-mm-thick lead (Fig. 1). X-ray irradiation was performed using a MBR-1520R X-ray generator (150 kV and 20 mA, Hitachi Medical Corporation, Tokyo, Japan). Con-G was subjected to a treatment

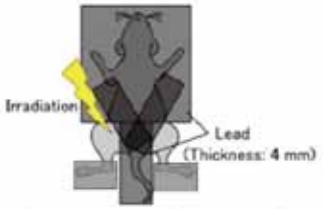

Fig1. Schema of X-irradiation to the rat

similar to 15 Gy-G and 30 Gy-G, except they were not exposed to X-ray irradiation.

To assess the changes in the hind limbs caused by X-ray irradiation over time, the body weight of each rat was measured the day before irradiation, and at 1 and 3 days, and 1, 2, 3, 4, 5 and 6 weeks after irradiation. On the same days, we also photographed the state of the hind limbs with a digital camera and measured the range of motion (ROM) for dorsiflexion of the ankle joint using the methodology previously reported [3, 4]. The ROM of the ankle joint was passively dorsiflexed maximally and measured by bending the rat hip and knee joints 90 degrees under anaesthesia. This 90 degree angle was defined as the angle formed by a line connecting the lateral malleolus and the centre of the knee joint to a line parallel to the bottom of the heel. Measurements were made at five-degree intervals using an angle meter. The spontaneous activity of each rat was measured once a week as the number of complete turns made on a Wheel Meter over a 24-hour period. At the end of the experimental period, all rats were sacrificed and their soleus muscles were extracted for wet weight measurements.

All procedures were carried out in accordance with the Guidelines for Animal Experimentation of our institution.

Results

In the 30 and 50 Gy-G, hair loss, tumours, and effusions of the hind legs were observed starting two weeks after irradiation. The tumours observed in the 50 Gy-G were more severe than those in the 30 Gy-G. Improvements in the masking method eliminated plantar injuries. (Fig. 2)

The weight of both the 30 and 50 Gy-G remained stable for three weeks after irradiation, and then increased. (Fig. 3)

The spontaneous activity and the ROM of dorsal flexion of both the 30 and 50 Gy-G decreased for 3 weeks after irradiation, then increased in the 30 Gy-G, but remained low in the

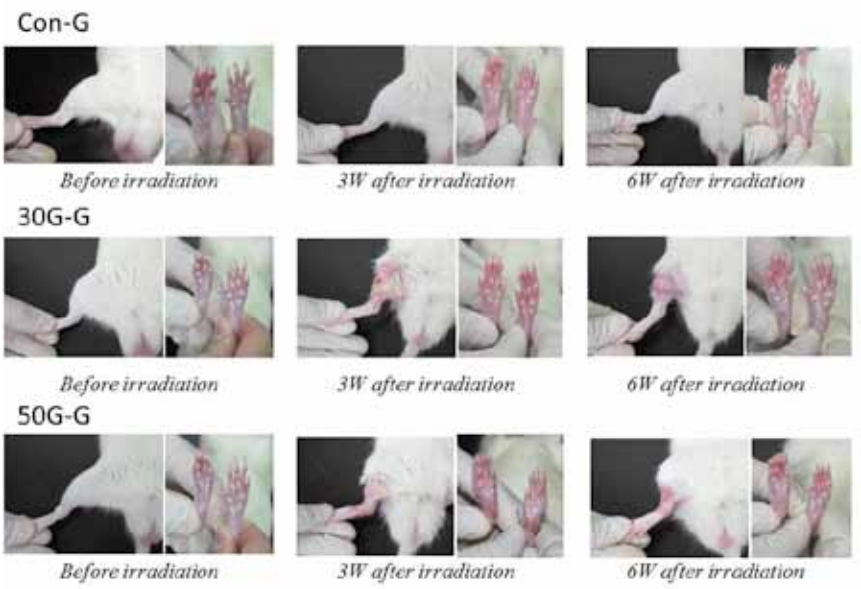

Fig2. State of hind limbs

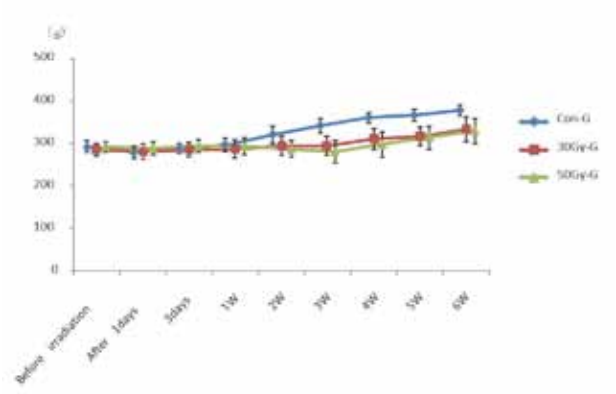

Fig3. Change in body weight

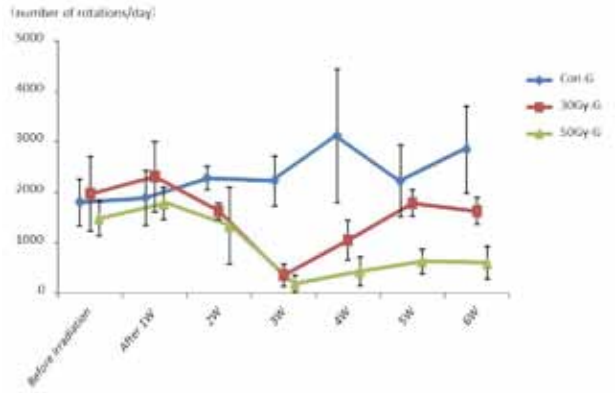

Fig4. Change in spontaneous activity

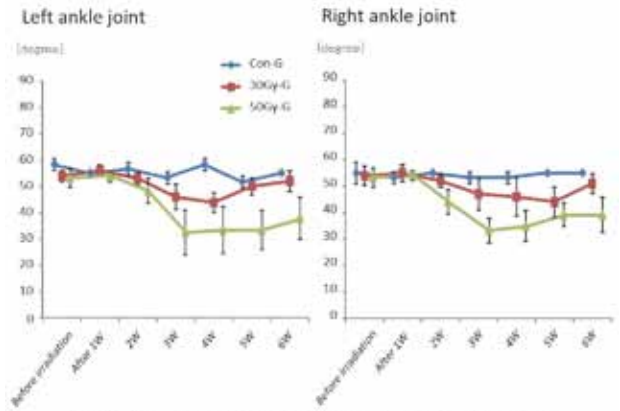

Fig5. Change in ROM of dorsiflexion of ankle joints

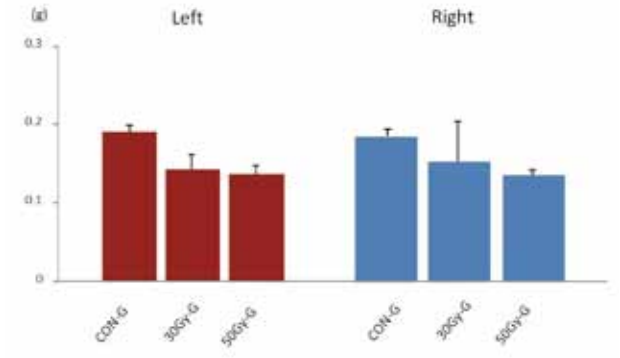

Fig6. Wet weight of soleus muscle

50 Gy-G. (Fig. 4) increased in the 30Gy-G while remaining low in the 50Gy-G. (Fig. 4)

The wet weights of the soleus muscle were lower in both the 30 and 50 Gy-G than in the Con-G. (Fig. 5)

Discussion

The results of our last report suggested that no adequate animal model for local radiation injury could be developed, since X-ray irradiation at 15 Gy caused few changes in the animal model that

reflected clinical conditions [5]. Specifically, a level of X-ray irradiation was required to inhibit satellite cells. It had been hypothesized that the activity of satellite cells, which are important to the regeneration of skeletal muscle, are inhibited when irradiated with high-dose radiation [6]. Preliminary research indicated that X-ray irradiation of 25 Gy or more was necessary to inhibit satellite cells [7]. In the current study, we collected data at two X-ray exposure doses and here report on the progress and problems of developing an animal model.

The clinical condition of the 50 Gy-G was carefully observed and found to remain stable throughout the study period, whereas the clinical condition of 30 Gy-G changed during the study period as follows: spontaneous activity increased 3 weeks after irradiation, and major individual differences were apparent in the muscle wet weight of the soleus. Therefore, a radiation dose of at least 50 Gy is required to develop an animal model of local radiation damage. Concerning the reason that clinical manifestations of 30 Gy are unstable, we suspected that the transmission of radiation was inhibited due to the significant amounts of fluid present in the hind-limb tissues. Therefore, we speculate that satellite cells might not have been destroyed because most of the radiation was absorbed by the skin and thus not able to penetrate to the muscle. Indeed, skin injuries similar to those reported in the preliminary research of Modular et al. [8] and Kaneko et al. [9] were observed following radiation exposure to 30 Gy or more. Histopathological examination of the soleus and skin is required to clarify this point and will be conducted in future.

Conclusion

This study was conducted to study the processes and problems of developing an animal model of local radiation damage of the hind limbs. The clinical condition of the 50 Gy-G was carefully observed and found to remain stable throughout the study period. Therefore, a radiation dose of 50 Gy or more is necessary to develop an animal model of local radiation damage. Additionally, there was a clear difference between con-G and 50 Gy-G, particularly in the spontaneous activity and ROM of the ankle joint. Therefore, values for spontaneous activity and ROM of the ankle joint may become valid indices of radiation exposure in an animal model.

In the future, we would like both to investigate the histopathology of the soleus muscle and skin and to collect normative data regarding this animal model of local radiation damage. We also believe it necessary to test the effects of rehabilitation interventions.

References

[1] Narita H, et al.: Considering necessity and feasibility of rehabilitation for radiation-exposed patients from literature review. J Health Sci Res 1: 49-54 (2011).

[2] Koeda S, et al: Necessity and possibility of rehabilitation for patients exposed to radiation. Investigation by literature review. Med Biol 155(4):203-209(2011). (in Japanese)

[3] Okita M, et al.: Effects of short duration stretching on disuse muscle atrophy in immobilized rat soleus muscle. J Jpn Phys Ther Assoc 4:1-5(2001).

[4] Ono T, et al.: The effect of ROM exercise on rats with denervation and joint contracture. J Phys Ther Sci 21:173-176(2009).

[5] Narita H, et al: The effect of rehabilitation on large dose radiation damage to the skin and muscle -Developing an animal model of local radiation damage of the hind limbs-. The proceedings of the 4th International Symposium on Radiation Emergency Medicine in Hirosaki University: 47-50(2012).

[6] Ambrosio F, et al.: The effect of muscle loading on skeletal muscle regenerative potential: an update of current research findings relating to aging and neuromuscular pathology. Am J Phys Med Rehabil 88:145-155(2009).

[7] Rosenblatt JD, et al.: Gamma irradiation prevents compensatory hypertrophy of overloaded mouse extensor digitorum longus muscle. J Appl Physiol 73:2538-43(1992).

[8] Phelan JN, et al.: Effect of radiation on satellite cell activity and protein expression in overloaded mammalian skeletal muscle. Anat Rec 247:179-188(1997).

[9] Kaneko, et al.: Relationship between measurements of blood oxidative metabolites and skin reaction in irradiated rats. Yamagata Med J 29:19-288(2011). (in Japanese)

Elucidation of the mechanism of immunoregulation after double-unit umbilical cord blood transplantation

Izumi Nanba[1], Yuka Tamoto[1], Koichi Terashima[1], Hiroshi Maeda[2], Manabu Nakano[2], Kyoko Ito[2], and Koichi Ito[2*]

[1]Department of Medical Technology, Hirosaki University School of Health Sciences
[2]Department of Biomedical Sciences, Division of Medical Life Sciences, Hirosaki University Graduate School of Health Sciences

Abstract. Umbilical cord blood cell (UCBC) transplantation is an effective treatment to counter the lethal effects of whole-body irradiation. Furthermore, double-unit UCBC (dUCBC) transplantation is a more effective strategy to achieve steady hematopoietic recovery. However, immunological analysis involved in hematopoietic reconstitution by dUCBC is not fully conducted. In this study, we analyzed the characteristics of immune reconstitution induced by dUCBC transplantation by using a murine model. An MHC-matched single unit in dUCBC transplantation preferentially reconstituted the recipient's immune system. Hematopoietic recovery with recipients' own hematopoietic stem cells (HSCs) was achieved in fully allogeneic dUCBC transplantation. We propose that memory-type cytotoxic T lymphocytes (CTLs) of the recipient marrow likely participate in these selective regulations.

Key Words: double-unit umbilical cord blood transplantation, hematopoietic stem cell, memory T cell

Introduction

Currently, umbilical cord blood cells (UCBCs) are favored as the primary source of hematopoietic stem cells (HSCs) for transplantation [1,2]. However, the limited quantity of cord blood samples that can be obtained from a single donor hampers UCBC transplantation. Double-unit UCBC (dUCBC) transplantation has emerged as an effective strategy to overcome the limitations of cord blood transplantation [3-6]. Owing to a lack of suitable animal models, analyses of the differentiation capacity of dUCBCs in recipients have been limited to clinical observations [5]. In the present study, we evaluated the characteristics of immune reconstitution and the immunoregulatory mechanism involved in HSC engraftment following dUCBC transplantation in mice. Specifically, we examined the role of alloreactive memory $CD8^+$ T cells in the regulation of HSC engraftment in the recipients' bone marrow (BM).

Materials and Methods

dUCBC transplantation

Natural killer cells were depleted from wild-type female C57BL/6 (B6) ($H\text{-}2^b$) recipient mice by intraperitoneal administration of rabbit anti-asialo GM1 polyclonal antibody, one day before the transplantation. On the following day, lethally X-ray-irradiated B6 ($H\text{-}2^b$) mice received transplants of 1 of the following combinations of dUCBC: Group (1), GFP-Tg B6 ($H\text{-}2^b$) and C3H

* Corresponding to: Koichi Ito, Professor, Hirosaki University Graduate School of Health Sciences, 66-1 Hon-cho, Hirosaki, 036-8564, Japan.
E-mail: kohito@cc.hirosaki-u.ac.jp

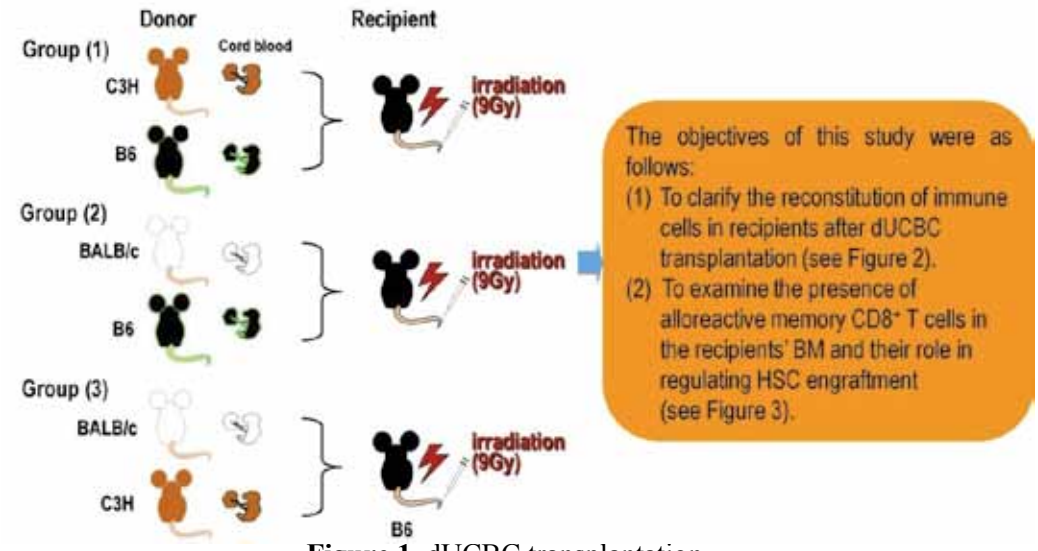

Figure 1. dUCBC transplantation

(H-2^k); Group (2), GFP-Tg B6 (H-2^b) and BALB/c (H-2^d); and Group (3), C3H (H-2^k) and BALB/c (H-2^d), with each combination containing an equal number of cells. At 16 weeks post-transplantation, the reconstitution of the newly developed immune system was assessed in the recipients. The experimental procedure was approved by the Animal Research Committee of Hirosaki University, and performed in accordance with the Institutional Guidelines for Animal Experimentation.

Results

Reconstitution of immune cells by dUCBC transplantation

At 16 weeks post-transplantation, hemato-poietic reconstitution of the recipient's immune system was analyzed by flow cytometry, utilizing specific antibodies against the lineage markers CD3 (T cells), CD45R/B220 (B cells), CD11b (macrophages), and Ly-6G (granulocytes). The donor origin of each lineage population was determined by staining with anti-H-$2K^k$ (for C3H) and /or H-$2K^d$ (for BALB/c) antibody. GFP^+ lineage cells were identified as of B6 donor origin. The survival rate 16 weeks post-transplantation was 92% (12/13) for Group (1), 73% (8/11) for Group (2), and 50% (3/6) for Group (3) (data not shown). Bar graphs in Figure 2A show the percentage of reconstituted cells of each lineage in the peripheral blood. Our analysis revealed that donor UCBCs differentiated into T cells, B cells, monocytes, and granulocytes in all recipients. The pie chart shows the proportions of donor MHCs in each of the recipient's lineage population analyzed. In the mice that received transplants of Group (1) or (2), the MHC-matched single units from GFP-Tg B6 were the sole source of long-term hematopoiesis, indicating that allogeneic HSCs were eliminated. However, in mice that received transplants of Group (3), hematopoiesis was reconstituted by the B6 recipients' own X-ray-resistant HSCs. Interestingly, hematopoiesis was restored by HSCs derived from BALB/c but not those from GFP-Tg B6 in T-cell-deficient Rag2(-/-) B6 recipients and in mice that received dUCBC transplants of Group (2) (Figure 2B). These results suggest that alloreactive T cells likely participate in allogeneic HSC elimination in wild-type B6 recipients.

Allo-MHC reactive memory T cells in bone marrow

Since the BM forms a specialized micro-environment that supports HSC survival, we speculated that alloreactive T cells in the recipient's BM play a key role in the elimination of allogeneic HSCs. To examine this possibility, we first analyzed BM and spleen cells from normal B6 mice by flow cytometry. We found that the proportion of $CD44^{high+}$ cells (indicating the memory type) within $CD4^+$ or $CD8^+$ cell populations was higher in the BM (90% in $CD4^+$ and 46% in $CD8^+$) than in the spleen (65% in $CD4^+$ and 36% in $CD8^+$) or peripheral blood (28% in $CD4^+$ and 11% in $CD8^+$) (Figure 3A). Thus, BM-resident T cell population is rich in memory-type cells and differs from splenic or peripheral blood T cells.

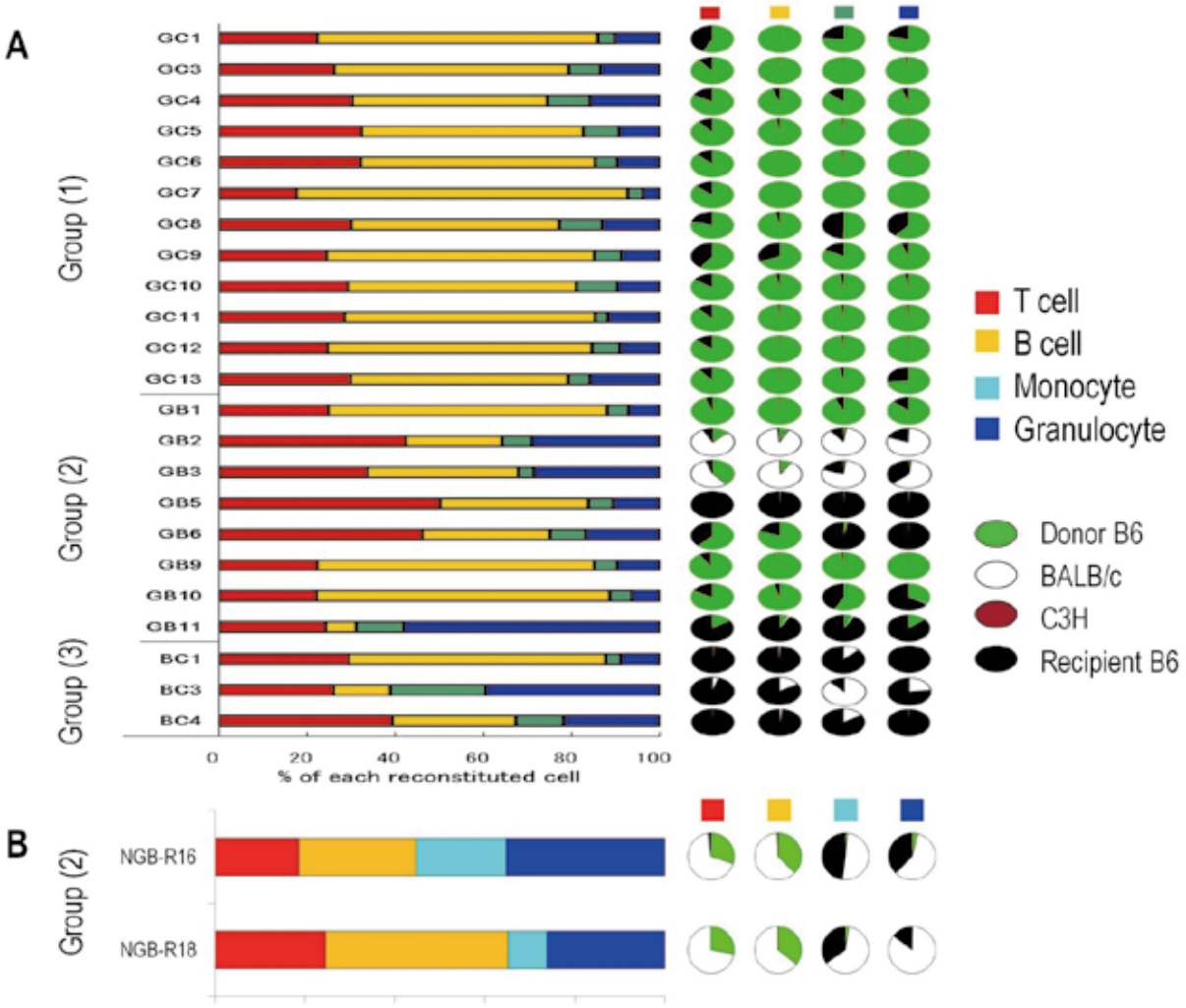

Figure 2. Reconstitution of immune cells by dUCBC transplantation

Next, we investigated the alloreactivity of the accumulated memory $CD8^+$ T cells in the recipient's BM. Normal B6 mice were transplanted twice with the skin from BALB/c or B6 (control) to generate alloreactive cytotoxic T lymphocytes (CTLs). One month after a second BALB/c-skin graft rejection, the cytolytic activities were examined using a chromium release assay on T lymphoma (A20.2J) from BALB/ mice, and B lymphoma (EL4) from B6 mice. As shown in Figure 3B, strong alloreactive killing activity against BALB/c (A20.2J) was detected in BM and spleen cells of the BALB/c-skin-grafted B6 mice, and not in B6-skin-grafted B6 mice. The results indicate the presence of alloreactive memory T cells in the BM. In contrast, no killing activity was observed when EL4 was used as target cells.

Conclusions

Our results indicate that alloreactive T cells in the BM of mice receiving dUCBC transplants may participate in preferential selection of MHC-matched UCBC during hematopoietic reconstitution. Finally, whether T-cell-deficient Rag2 (-/-) B6 mice receiving memory $CD8^+$ T cells derived from the BM of B6 mice can show recovery of the hematopoietic activity of GFP-Tg B6 HSC from dUCBC transplants of Group (1) or (2) needs to be further examined.

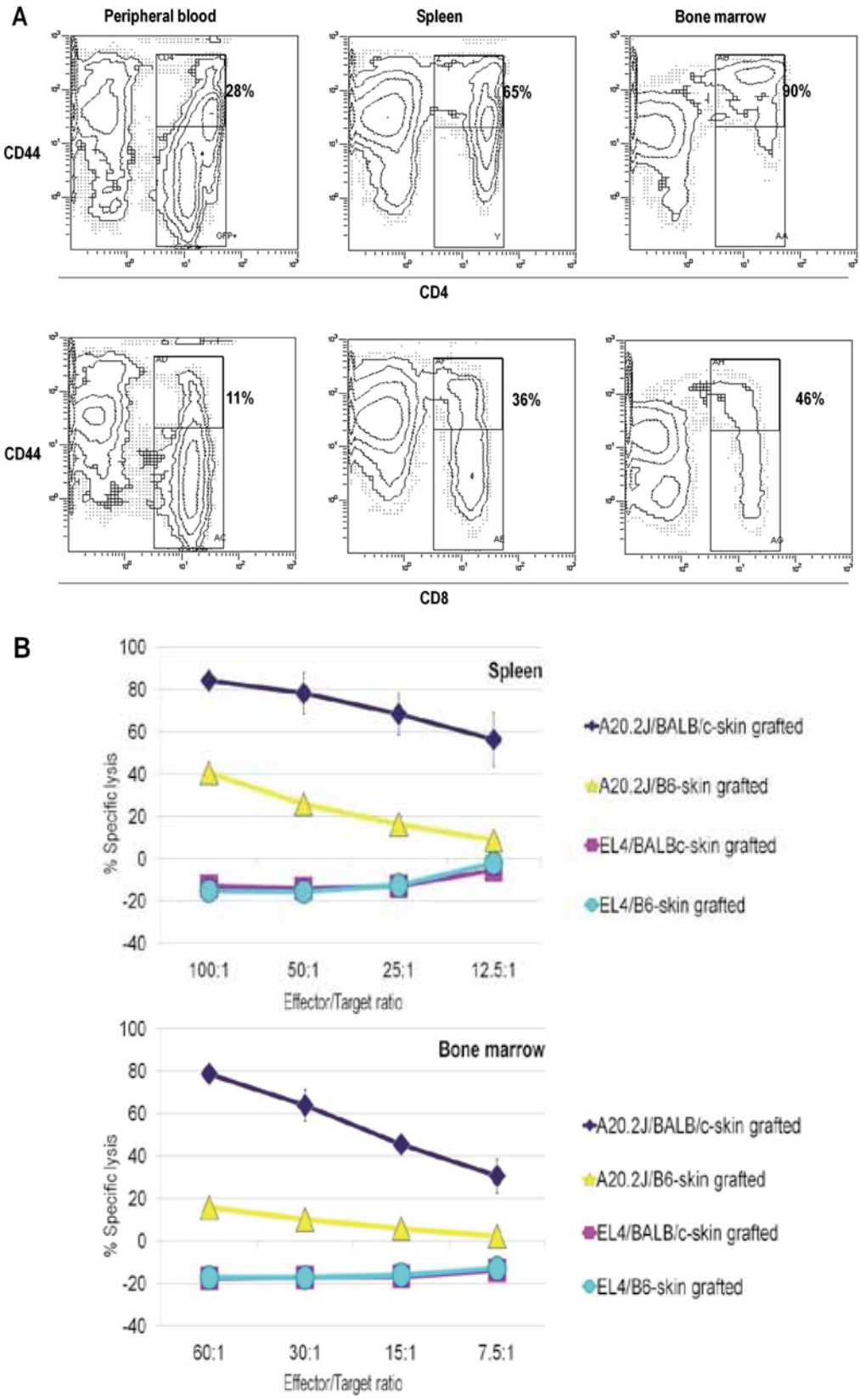

Figure 3. Allo-MHC reactive memory T cells in bone marrow

References

[1] Atsuta, Y, Morishima Y, Suzuki R, et al. Comparison of unrelated coed blood transplantation and HLA-mismatched unrelated bone marrow transplantation for adults with leukemia. *Biol Blood Marrow Transplant* 2012; 18: 780-787.

[2] Locatelli F, Kabbara N, Ruggeri A, et al. Outcome of patients with hemoglobinopathies given either cord blood or bone marrow transplantation from an HLA-identical sibling. *Blood* 2013; 122: 1072-1078.

[3] Newall LF, Milano F, Nicoud IB, et al, Early CD3 peripheral blood chimerism predicts the long-term engrafting unit following myeloablative double-cord blood transplantation. *Biol Blood Marrow Transplant* 2012; 18: 1243-1249.

[4] Milano F, Heimfeld S, Gooley T, et al. Correlation of infused CD3+CD8+ cells with single-donor dominance after double-unit cord blood transplantation. *Biol Blood Marrow Transplant* 2013; 19: 156-160.

[5] Ponce DM, Gonzales A, Lubin M, et al. Graft-versus-host disease after double-unit cord blood transplantation has features and an association with engrafting unit-to-recipient HLA match. *Biol Blood Marrow Transplant* 2013; 19: 904-911.

[6] Somers JA, Brand A, van Hensbergen Y, et al. Double umbilical cord blood transplantation: a study of early engraftment kinetics in leukocyte subsets using HLA-specific monoclonal antibodies. *Biol Blood Marrow Transplant* 2013; 19: 266-273.

Effect of the concomitant use of 4-methylumbeliferone and radiation on human fibrosarcoma cells

Ryo Saga[1], Yoichiro Hosokawa[1], Hironori Yoshino[1], Shingo Terashima[1], and Toshiya Nakamura[2]

Departments of [1]Radiological Technology Science and [2]Medical Technology
Hirosaki University School of Health Sciences
66-1 Hon-Cho, Hirosaki, Aomori, 036-8564 Japan

Abstract. In this study, we examined the effects of the concomitant use of radiation and 4-methylumbelliferon (MU) on metastasis. HT1080 cells were prepared to provide a Control group, a DMSO group, an MU group, an irradiation-alone group, and an MU + irradiation group. Comparison of the MU group and the DMSO group showed a significant decrease in hyaluronan concentrations in the culture supernatant of the MU group. Moreover, comparison of the MU + irradiation and irradiation-alone groups showed a significant decrease in hyaluronan concentration in the culture supernatant of the MU+ irradiation group. In the invasion assay, a significant decrease in the invasion rate was observed in the MU + irradiation group. Zymography showed that the bands added with MU were relatively decreased. The addition of MU resulted in a decrease in hyaluronan concentration, invasion rate, and both matrix metalloproteinase 2 (MMP2) and matrix metalloproteinase 9 (MMP9). These trends were significant following irradiation. Therefore, following irradiation, MU reduces hyaluronan production and prevents metastasis.

Introduction

4-Methylumbelliferon (MU) inhibits hyaluronan synthesis. Hyaluronan, the main component of the extracellular matrix, is synthesized in excess in cancer tissues. The synthesis of hyaluronan is closely related to invasion and metastasis of cancer. However, the effects of MU with the concomitant use of radiation remain unknown. In this study, we examined the effects of the concomitant use of radiation and the inhibitory effect of MU on metastasis.

Methods and Materials

The human fibrosarcoma cell line, HT1080, was purchased from ATCC (USA). HT1080 cells were irradiated and prepared to provide a Control group, a DMSO group, an MU group, an irradiation group, a DMSO + irradiation group, and an MU + irradiation group. MU was dissolved in DMSO, and all groups were administered the same ray generator (HITACHI, Japan). Irradiation conditions were 2 Gy at 150 kV, 20 mA, and a rate of 0.9 Gy/min. The cells were stained with trypan blue. Hyaluronan in the culture supernatant was concentration of DMSO (0.1 mM or 0.5 mM). The cells were incubated at 37°C for 24 hours in a 5% CO_2 environment after administration of DMSO and MU, and irradiated using a MBR-1520R-3 X-measured using a Hyaluronan Quantikine ELISA Kit (RD System, USA). Hyaluronan levels were calculated from the absorbance obtained using a microplate reader. The invasion assay was conducted using a BioCoat Matrigel Invasion Chamber (BD, USA). The invasion cells were fixed and stained using a Diff-Quik staining kit. The number of cells within a predetermined field of view (876 μm × 659 μm) were counted, allowing calculation of the invasion rate: Invasion rate = (number of invasion cells) / (number of migrated cells) × 100. MMP2 and MMP9 (matrix metalloproteinase) were measured using zymography. A serum-free culture medium was used, and band size was determined by gel densitometry using the program Image J.

* Correspondence to: Yoichiro Hosokawa, Professor, Hirosaki University Graduate School of Health Sciences, 66-1, Hon-cho, Hirosaki 036-8564, Japan E-mail: hosokawa@cc.hirosaki-u.ac.jp

Results and discussion

Fig. 1 shows the hyaluronan concentration obtained from the measured absorbance. The difference in hyaluronan concentration between the Control and irradiation-alone groups was not statistically shown.

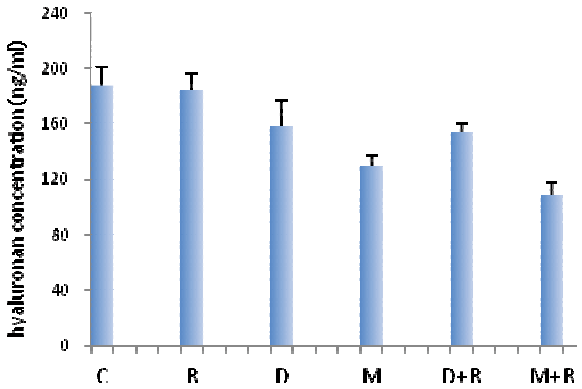

Fig 1. hyaluronan concentration
(C = control, R = radiation, D =DMSO0.1mM, M =MU 0.1mM, D+R =DMSO 0.1mM + radiation, M+R =MU 0.1mM + radiation)

Comparison of the DMSO, Control, and MU (0.1 mM) administered groups showed that hyaluronan concentration was significantly decreased in both the MU administered-alone and MU + irradiation groups (Fig.1). These results reveal that MU administration decreases the production of hyaluronan, even if cells are irradiated.

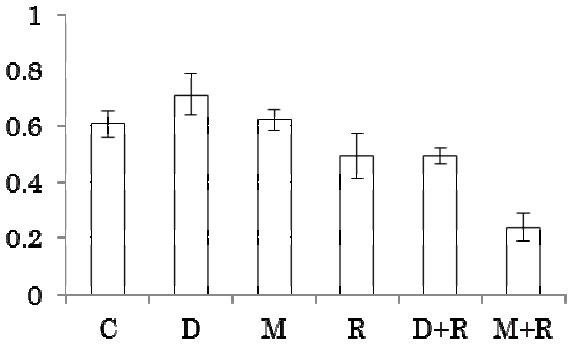

Fig 2. invasion rate
(C = control, R = radiation, D =DMSO 0.1mM, M =MU 0.1mM, D+R =DMSO 0.1mM + radiation, M+R =MU 0.1mM + radiation)

Fig. 2 shows the invasion rate calculated from the invasion assay results and the number of cells measured. A significant decrease was observed in the MU administered-alone compared to DMSO groups, and a significant decrease was seen in the MU + irradiation group compared to irradiation-alone. These results reveal that MU administration inhibits the invasion activity of cells, even if the cells are irradiated. Fig. 3 shows the results of absorption measurements on MMP2 and MMP9.

Fig 3. Zymography
(C = control, R = radiation, D =DMSO 0.1mM, M =MU, D+R =DMSO 0.1mM + radiation, M+R =MU + radiation)
(0.1 = 0.1mM MU, 0.5 = 0.5mM MU)

Fig. 4 and Fig. 5 reveal the areas quantified by densitometry measurements. The bands caused by the presence of MU were somewhat decreased when we compared the DMSO and MU administered groups with the irradiation-alone and MU + irradiation groups. Although there were no statistical differences, these results suggested that MU might reduce breakage of the cell membrane by cancer cells by MMP2 and MMP9.

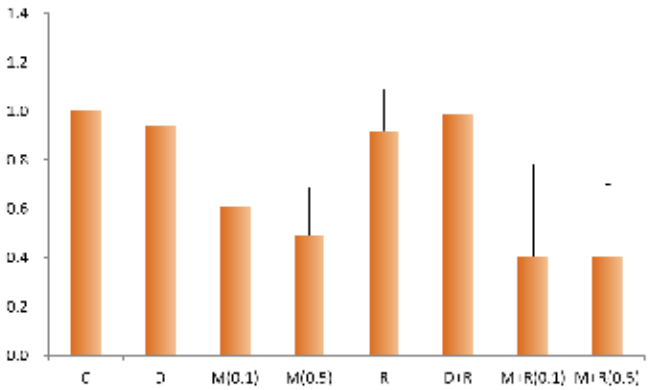

Fig 4. density rate of MMP9

(C = control, R = radiation, D =DMSO 0.1mM, M =MU, D+R =DMSO 0.1mM + radiation, M+R =MU + radiation)
(0.1 = 0.1mM MU, 0.5 = 0.5mM MU)

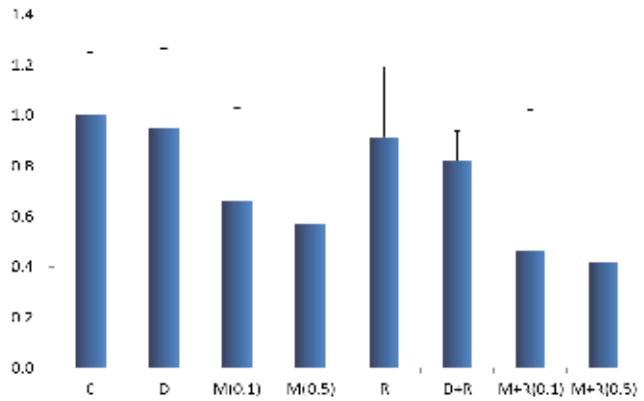

Fig 4. density rate of MMP2

(C = control, R = radiation, D =DMSO 0.1mM, M =MU, D+R =DMSO 0.1mM + radiation, M+R =MU + radiation)
(0.1 = 0.1mM MU, 0.5 = 0.5mM MU)

Conclusions

The addition of MU decreases both hyaluronan concentration and the invasion rate, and also a tendency to reduce MMP2 and MMP9 levels. This trend was more significant following irradiation. Thus, following irradiation, MU reduces hyaluronan production and prevents metastasis.

References

1．Okuda H，Kobayashi A，Xia B，他．Hyaluronan synthase HAS2 promotes tumor progression in bone by stimulating the interaction of breast cancer stem-like cells with macrophages and stromal cells　2012; 72(2): 537-47.

Low dose dependence of sucrose radical generation

Yuzuru Sato[1], Kouichi Nakagawa[2,*] and Takuto Takahashi[1]

[1]Department of Radiological Sciences, Hirosaki University, Hirosaki, Japan
[2]Department of Radiological Life Sciences, Division of Medical Life Sciences, Hirosaki University Graduate School of Health Sciences, Hirosaki, Japan

Abstract. We investigated stable radicals produced by low dose X-ray irradiation of sucrose. The sucrose radicals were detected by electron spin resonance (ESR) at ambient temperature. The ESR signal intensity of the radicals is proportional to the accumulated dose and increases linearly with increasing absorbed dose. In addition, we examined the effect of dose rate (0.5 Gy/min to 1.5 Gy/min) on the ESR signal intensity of irradiated sucrose and found no dose rate dependence for the stable radical production. Thus, the present ESR results for low dose irradiation provide new insights into a possible sucrose ESR dosimeter.

Key Words: ESR, sucrose, X-ray low dose, radical, irradiation

[*]Correspondence to: Kouichi Nakagawa, Professor
Hirosaki University, 66-1 Hon-cyo, Hirosaki 036-8564, Japan
E-mail: nakagawa@cc.hirosaki-u.ac.jp

Introduction

The interaction between materials and radiation is an important subject in radiological science [1]. Stable radicals produced due to radiation-material interactions can be reliably measured by Electron Spin Resonance (ESR) spectroscopy [1,2]. The stability of the radicals is associated with the dose accumulation. Moreover, the stability of the radical can be affected by environmental variables such as humidity. However, this is generally easy to control. Thus, ESR spectroscopic technique is the most reliable method to measure the radicals [1,2].

We studied the effects of low dose X-ray irradiaton on polycrystalline sucrose using ESR in order to find how low-dose rradiation produces stable radicals. We also examined the effect of dose rate dependence on ESR intensity of the irradiated sucrose. The results are discussed in terms of a sucrose dosimeter.

Experimental

Sample preparation

Sucrose (molecuar weight, 342) was purchased from Wako Pure Chemical Industries, Ltd., Tokyo, Japan and used as received. Each polycrystalline sample (0.50 g) was wrapped with a plastic sheet to allow uniform irradiation. A sample quantity of 0.50 g was chosen to have optimum ESR signals in an cavity.

X-ray low dose irradiation

Samples were irradiated using a HITACHI MBR-1520R X-ray instrument (Ibaragi, Japan) at 150 kV and 20 mA. Three different dose rates (0.5, 1.0, and 1.5 Gy/min) were used. Low energy radiation was filtered using a 0.3 mm copper and 0.5 mm aluminum filter. Doses of 0.25, 0.5, or 1.0 Gy were delivered stepwise. All irradiated samples were kept at ambient temperature for one day before ESR measurements.

ESR measurements

The irradiated samples were put into standard ESR tubes (o.d. 4.7 mm, i.d. 3.6 mm, JEOL Datum Co., Tokyo, Japan). The induced radicals were measured using a JEOL RE 3X 9 GHz ESR spectrometer at least 24h after the irradiation. The resonance frequency was measured using a microwave frequency counter (EMC-14, Echo Electronics Co., Ltd., Tokyo, Japan). All irradiation and measurement processes were carried out at ambient temperatures [2-6].

Results and Discussion

Figure 1 shows single scan ESR spectra obtained at ambient temperature. The ESR is able to observe the signal from sucrose irradiated with the very low dose. Each ESR spectrum was obtained at the single scan.

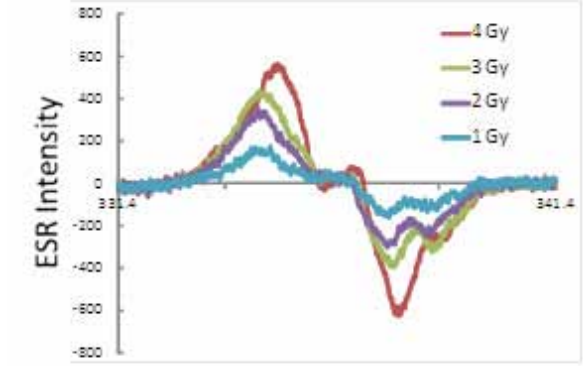

Figure 1. ESR spectra of irradiated sucrose obtained at doses of 1, 2, 3 and 4 Gy.

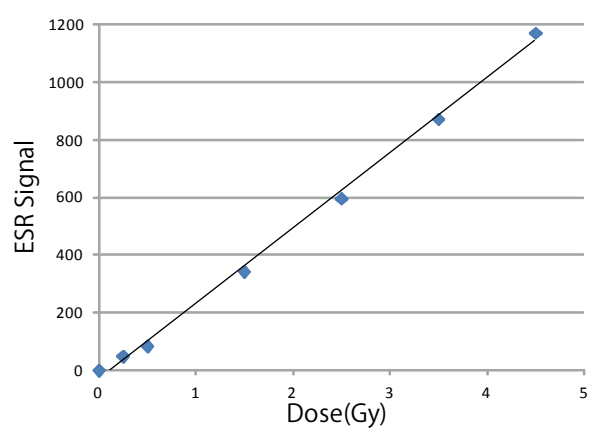

Figure 2. ESR signal intensity as a function of the absorbed dose.

Figure 2 shows shows ESR signal intensity as a function of the absorbed dose. The ESR signal intensity increases linearly with increasing the absorbed dose. The tendency was observed at very low dose. The results are advantageous as an ESR dosimeter.

In addition, we have examined the ESR intensity regarding dose rate dependence of the irradiated sucrose. The dose rates were changed from 0.5 Gy/min to 1.5 Gy/min. The ESR intensity increases linearly with increasing the absorbed dose as shown in Figure 3. The results indicate that there is no dose rate dependence for the stable radical production.

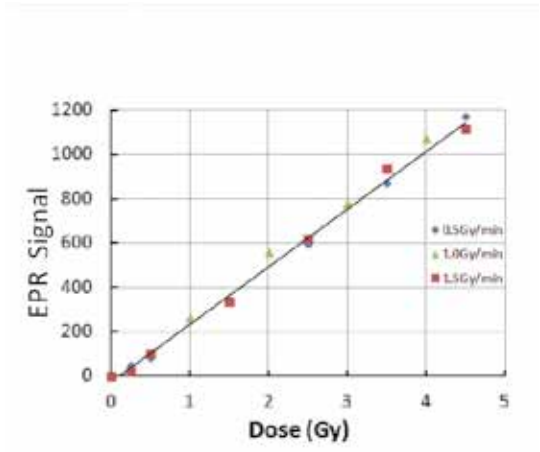

Figure 3. ESR signal intensity as a function of various dose rates: 0.5, 1.0, and 1.5

Finally, we investigated low dose irradiation of sucrose for the first time. The ESR signal intensity is proportional to the accumulation of the doses. There is no dose rate dependence for the stable radical production. Therefore, the present ESR investigation of the low-dose irradiation of sucrose provides new insights regarding the sucrose ESR dosimeter.

References

[1] Nakajima, T., Otsuki T., Dosimetry for radiation emergencies: radiation-induced free radicals in sugar of various countries and the effect of pulverizing on the ESR signal. *Appl. Radiat. Isot*. 41: 359-365 (1989).

[2] Nakagawa, K., Nishio, T., 2000. Electron Paramagnetic Resonance Investigation of Sucrose Irradiated with Heavy Ions, *Radiat. Res.*, **153**, 835-839 (2000).

[3] Nakagawa K., Sato Y.: Investigation of Heavy-Ion Induced Sucrose Radicals by Electron Paramagnetic Resonance. Radiat. Res. **164**, 336-338 (2005).

[4] Nakagawa, K., Sato, Y, Analyses of the EPR responses of sucrose and L-α-alanine radicals induced by C, Ne, and Ar ion irradiations, Spectrochimca Acta, Part A, Mol. & Biomol. Spectroscopy, **63**, 851-854 (2006).

[5] Nakagawa, K., Ikota, N., Anzai, K., Sucrose and L-alanine radical-production cross section regarding heavy-ion irradiation. Spectrochim Acta Part A, 69, 1384-1387 (2008).

[6] Karakirova, Y, Nakagawa, K., Yordanov N. D., EPR and UV spectroscopic investigations of sucrose irradiated with heavy-ion particles, Radiat. Meas., 45, 10-14 (2010).

Acknowledgments

Part of this research was supported by a Grant-in-Aid for Exploratory Research (24650247) and for Scientific Research (B) (25282124) from Japan Society for the Promotion of Science (JSPS) (K.N.).

Biological dosimetry in large scale accidents

Andrzej Wojcik

Centre for Radiation Protection Research,
Stockholm University, Sweden

In the event of a large scale radiological emergency biological dosimetry is an essential tool that can provide timely assessment of radiation exposure to the general population and enable the identification of those exposed people, who should receive immediate medical treatment. A number of biodosimetric tools are potentially available, but they must be adapted and tested for a large-scale emergency scenario. These methods differ in their specificity and sensitivity to radiation, the stability of signal and speed of performance. A large scale radiological emergency can take different forms. Based on the emergency scenario different biodosimetric tools should be applied so that the dosimetric information can be made available with optimal speed and precision.
The FP7 Security program of the European Commission funded a multi-disciplinary collaborative project where we analysed a variety of biodosimetric tools and adapted them to different mass casualty scenarios. The assays were chosen because to complement each other with respect to sensitivity, specificity to radiation and the exposure scenario as well as speed of performance.
The project involved the key European players with extensive experience in biological dosimetry and finished in April 2013. Training was carried out and automation and commercialisation pursued. An operational guide was developed and disseminated among emergency preparedness and radiation protection organisations. The main achievements and conclusion from the project will be presented.
The project was funded by the FP7 Security program. URL: http://www.multibiodose.eu.

Acute radiation syndrome caused by accidental radiation exposure - therapeutic principles

Harry Scherthan

Bundeswehr Institute of Radiobiology affiliated to the University of Ulm, Neuherbergstr. 11, D-80937 Munich, Germany

E-mail: scherth@web.de

Management of the Acute Radiation Syndrome (ARS) still remains a challenge. There is a strong need for preparatory planning including the allocation of scarce resources, such as specialized hospital treatment capacities and stockpiling of specific medical countermeasures. A key problem when facing preparedness for radiation accidents is the fact that only very limited treatment options have really been tested in clinical settings and therefore the evidence of many treatment modalities still is low. Evidenced based recommendations will be presented and discussed. Moreover there are new treatment options under development, which show promising results either at pre-clinical development stages or when administered in case studies. Among these are mesenchymal stem cells of different origin, which can add a significant value to already established therapeutic regimens both for the treatment of localized radiation injuries and for a treatment of whole body exposures. The current literature will be reviewed and future perspectives will be shown.

When facing the situation of an accidental whole body or significant partial body exposure the role of multi-organ involvement and multi-organ failure always has to be addressed. Only an understanding of these key pathophysiological principles can help to develop causal oriented treatment principles. This aspect also includes new diagnostic tools to visualize and document multi-organ damage in the living system. A new pilot approach will be presented.

Use of mesenchymal stromal cells in treating radiation-induced lesions: principle and practice

Marc Benderitter

IRSN, PRP-HOM/SRBE, Laboratory of Radiopathology and Experimental Therapies-FRANCE
E-mail: chiaki@cc.hirosaki-u.ac.jp

Effect of radiation on healthy tissue. IRSN is strongly implicated in the field of regenerative medicine of healthy tissue after severe radiation damages.

Regenerative medicine based on stem cell injection as a medical countermeasure in case of severe radiation burns: a clinical transfer. Recently, in collaboration with the Percy hospital (Clamart, France) our group have evidenced for the first time, the efficiency of MSC therapy in the context of acute cutaneous and muscle damage following accidental exposure. Treatment of severe radiation burns remains a difficult medical challenge. The most severe manifestations are highly invalidating. Although several therapeutic strategies have been used with some success, none have proven entirely satisfying. The concept that stem cell injections could be used for reducing normal tissue injury has been discussed for a number of years. Pre-clinical and clinical benefits of mesenchymal stem cell injection for ulcerated skin and muscle restoration after high dose radiation exposure have been successfully demonstrated. Up to ten patients suffering from severe radiological cutaneous syndrome were successfully treated in France based on autologous human grade mesenchymal stem cell injection combined to plastic surgery or skin graft.

Mesenchymal stem cell in the treatment of severe radiation pelvic disease: towards clinical application. Radiotherapy may induce irreversible damage on healthy tissues surrounding the tumour. It has been reported that the majority of patients receiving pelvic radiation therapy shows early or late tissue reactions of graded severity as radiotherapy affects not only the targeted tumor cells but also the surrounding healthy tissues. The late adverse effects of pelvic radiotherapy concern 5 to 10% of them, which could be life threatening. However, a clear medical consensus concerning the clinical management of such healthy tissue sequelae does not exist. Although no pharmacologic interventions have yet been proven to efficiently mitigate radiotherapy severe side effects, few preclinical researches show the potential of combined and sequential pharmacological treatments to prevent the onset of tissue damage. Our group has demonstrated in preclinical animal models that systemic MSC injection is a promise approach for the medical management of gastrointestinal disorder after irradiation. We have shown that MSC migrate to damaged tissues and restore gut functions after irradiation. We carefully studies side effects of stem cell injection for further application in patients. The clinical status of three first patients suffering from severe pelvic side effects resulting from an overdosage was improved following MSC injection in a compationnal situation.

Stem cell therapy has now to be improved to the point that hospitals can put safe, efficient, and reliable clinical protocols into practice.

The 2013 Hirosaki University International Symposium

The Proceedings of the 5th International Symposium on Radiation Emergency Medicine at Hirosaki University

平成２６年　３月２２日　　印刷
平成２６年　３月２７日　　発行

編　集　　弘前大学大学院保健学研究科
〒036-8564　弘前市本町 66-1

印刷所　　やまと印刷株式会社